An antenna mount for tracking geostationary satellites

Eindhoven University of Technology
Netherlands

Department of Electrical Engineering

AN ANTENNA MOUNT FOR TRACKING GEOSTATIONARY SATELLITES

by

J. Dijk, E.J. Maanders and
J.M.J. Oostvogels

TECHNISCHE HOGESCHOOL EINDHOVEN
NEDERLAND
AFDELING DER ELEKTROTECHNIEK

EINDHOVEN UNIVERSITY OF TECHNOLOGY
THE NETHERLANDS
DEPARTMENT OF ELECTRICAL ENGINEERING

AN ANTENNA MOUNT FOR TRACKING GEOSTATIONARY SATELLITES

by

J. Dijk, E.J. Maanders and
J.M.J. Oostvogels

TH-Report 77-E-74
ISBN 90 6144 074 2

May 1977

page

Contents

Summary

This report deals with some electrical and mechanical aspects of an antenna mount which may be used for any geostationary satellite, preferably operating at frequencies between 10 and 60 GHz.

The report describes the requirements and conditions of such antenna systems and explains the severe requirements that result from the re-use of frequency principle at these frequencies.

Some mechanical principles that have been introduced in the antenna mount are discussed.

The mount is limited steerable with an azimuth range of 20 degrees and an elevation range of 10 degrees. If observations of one satellite are finished it is possible by a very simple arrangement to let the antenna point towards a different geostationary satellite. Coordinate transformations are given.

Experiences are obtained being involved in ATS-6 millimeter experiment. From these experiences some proposals are made for further improvement of the antenna system.

1. Introduction

Long distance line of sight communication is limited by the curvature of the earth and the height of the towers containing transmit and receive antennas. In the past systems have been developped using ionosphere and troposphere to make telecommunication beyond the horizon possible. Well known is ionospheric reflection between 2 and 30 MHz and troposcatter at frequencies from 500 - 10000 MHz.

On August 12, 1960 a 100 foot diameter spherical balloon was placed in orbit around the earth by the National Aeronautics and Space Administration (NASA) to study the feasibility of providing long distance communication by means of reflecting from orbiting earth satellites. Since the launch of this Echo I satellite [1], this type of communication has developped tremendously. The Echo satellites have been followed by active satellites such as Telstar and Relay, all in an elliptical orbit around the earth.

In 1963 the first geostationary satellite Syncom [2] was launched. A geostationary satellite completes a 35,600 km altitude equatorial orbit in exactly 24 hours. If such a satellite is moving in the direction of rotation of the earth it will remain stationary with respect to an arbitrary point of observation on the earth. The first geostationary 24 hour communication satellite appeared to be very attractive and was soon followed by Early Bird [3], being the first of the generations of Intelsat Satellites [4], four generations of which have now been launched.

Some experimental geostationary satellites such as ATS-6, OTS and SIRIO are now available or will soon be available. One of the mean objects of these satellites is the investigation of frequency re-use above 10 GHz by polarisation diversity. For this reason both copolar and cross-polar signals have to be received and investigated under various weather circumstances.

The first experimental geostationary satellite received at Eindhoven University of Technology at a frequency of 30 GHz showed little disturbances with regard to the geostationary orbit. These disturbances are sinusoidal both in the direction of the tangent and the normal to the equatorial plane. The resulting movement seen from Eindhoven are Lissajous figures [Fig. 1], slowly changing and drifting away. The area covered by this additional satellite movement was generally limited to 3 degrees in elevation and 2 degrees in azimuth.

In general the daily movement of the satellite in elevation is larger than in azimuth direction. In the course of a few weeks the satellite drifts away a few

degrees and has to be reset in its original position by command from earth regularly. It will be made clear in the next section that the beamwidth of the available antenna is much smaller than this area so that tracking the satellite is necessary.
This report will deal with the design of an antenna mount which, together with a reflector antenna, is capable following every geostationary satellite in a limited area. For this purpose we will specify some important features of antenna and mount. [See also Photo 1].

2. Requirements and conditions

The pointing accuracy to be defined for a certain application is in close relationship with the antenna beamwidth. The beamwidth ϑ is usually defined at the 3 dB points of the mean beam. A rule of thumb is the expression

$$\vartheta = 60\ \lambda/D$$

D being the aperture antenna.
The antenna available at Eindhoven University is a 3 meter precision dish and is used at a frequency of 30 GHz (λ = 1 cm) for the ATS-6 project; in that case ϑ is about 0.2 degrees.
The maximum of the copolar signal is found in the middle of the 3 dB points on the antenna axis. Generally it is acceptable that the mispointing is not more than $0.1\,\vartheta$ which is 0.02 degrees in this example, resulting in a copolar signal decrease of not more than 0.1 dB.
Because of re-use of frequency severe requirements with regard to the cross-polarised signal must be introduced. Generally, in symmetrical reflector antennas the cross polarised lobes have a maximum in planes at 45° to the principal plane [4, p. 423]. If the entire antenna system is well designed, the cross-polar pattern reaches a minimum on the antenna axis where the copolar signal has its maximum [Fig. 2].
The experience has learned that, to avoid an unwanted increase of the cross-polar reception due to mispointing, more severe requirements are necessary. To remain as close as possible to the cross-polar "dip" on axis, the pointing accuracy should be about $\vartheta/30 \approx 0.007$ degrees for the 3 meter antenna at 30 GHz. To fullfill this condition the antenna mount must be equipped with a very accurate read-out system both for azimuth and elevation movements. Small

corrections around a certain antenna pointing position should be possible thus requiring a very sensitive steering system. In such a system hysteresis should be minimised, which may be obtained by letting the friction between the movable parts to be very low.
Measures have to be taken to prevent that the antenna weight or the wind pressure causes degradations in the order of 0.007 degrees. This may be obtained by an antenna mount fixed to a concrete pedestal.
Backlash is not allowed at all.
The range in which accurate antenna pointing is possible should be such that after an initial contact with the satellite has been established, all further individual small movements of the satellite may be followed. Further, arrangements should be available to change over from one geostationary satellite to the other. In Eindhoven, this movement has only to be made if the experiments with one satellite are finished and preparations have to be carried out to receive the next geostationary satellite e.g. from ATS-6 to OTS.
The satellite ATS-6 moves only a few degrees per day; therefore, the speed of motions of the antenna may be very slow.

3. Kinematic construction

The mount is statically determined, this being an important constructive principle applied in the construction. It means that a line in space is always defined by two points and a surface by three points. When four points are given to define a surface incompatible information may be introduced e.g. a chair with four legs on a smooth floor actually stands on three legs. When somebody wants to take place, the chair may be tilted from one leg to another. The plane containing the points of contact is not defined and deformation of the chair is possible.
Another principle explains that the angular rigidity of a construction is proportional to the square of the radius to which the construction is attached. In Fig. 3 it is shown in which way a turning bar is attached to a spring at radius L and a second one at radius L/2. In the first case a force P will remove the tip of the bar over a distance x. However, when the spring is mounted at radius L/2, the force P at the tip acts as a force 2P in the middle of the bar and extends a spring over a distance 2x. The tip of the bar will have a displacement of 4x. This proves that the angular rigidity is proportional to the square of the radius to which the spring is mounted.

It is clear that every metal part is in fact an eleatic element. Therefore, the former phylosophy is not only valid for springs, but in general for every attachement. It may be concluded that for accurate antenna pointing the reflector has to be supported by three very eccentric points, viz. located at the edge of the reflector. The same requirements are valid for fixing the complete mount to the ground. Besides stiffness of the construction, it is also advisable to mount the reflector on very eccentric points because a small rotation may cause a large displacement, e.g. an angle of 0.007 degrees may be obtained by displacing a point on a radius of 115 centimetres over a distance of 0.14 millimetre [Fig. 4].
This means that a rather inaccurate drive will be sufficient, providing that it is mounted on a large radius. A disadvantage is that the range of such a system is limited, but for the application with geostationary satellites only, this is no objection.
A third principle is based on the fact that using a bar for bending or torsion is less efficient than using it for forces parallel to its axis. There is a maximum value for the stress in each part of the metal and its maximum value is reached in every part when stresses are imposed in the axial direction. For bending or torsion only half of the material is used. In mechanical engineering this problem is reduced by replacing the torsion bar by a hollow pipe and replacing the massive bending beam by what is known as a H-proflie, in such a way that in both cases the unefficient central material is reduced. However, a better solution is a construction where only axial forces are used. This is obtained by using ball hinges at each end of the bars. These ball hinges can not conduct bending forces or torsion. In fact, this is ideal for constructing frame work. By dividing the frame in triangles, connected by ball hinges, all the acting forces can be resolved to axial forces along several bars.
Using the three constructive principles explained above, there are still several possibilities for the mount. The reflector needs two degrees of freedom for scanning purposes. Therefore, the first idea is to fix the reflector at three points by ball hinges: M, D and C. C and D are movable by lead screws CB and DA. At fixed lengths of both lead screws the reflector is fixed in the desired direction.
In general a fixed body is restricted in six degrees of freedom (3 translations and 3 rotations). But the reflector body supported by point M and bars BC and AD has only 5 restrictions because M restricts the reflector in three translations, and BC and AD each restrict the reflector only in one way (elongation

of BC and AD). Therefore, the reflector supported by point M and bars AD and BC is still movable. Hence, another bar is needed to restrict the final degree of freedom of the reflector. For this last bar two possibilities are interesting.

The first solution is a bar between E and F, where E is exactly between C and D and where F is chosen in the CDM plane in such a way that the angle FME is 90^{o}. This configuration has orthogonal axes because elongation of both BC and AD means a rotation around axis FM and movements of points C and D a rotation around EM. BC and AD should be symmetrical for having the same relation between elongation of the lead screw and rotation of the antenna. A disadvantage of this system however is that 7 ball hinges are needed [Fig. 5].

Therefore, a simpler system is possible choosing the third bar between B and D. This system only consists of 5 points. Figure 6 shows this final solution for the antenna mount, according the above mentioned constructive principles. The points A, B, C, D and M are all ball hinges. A, B and M are foundation points. The points C, D and M are connected to the parabolic reflector. Rotation of the antenna is possible by changing the length of the lead screws AD and BC.

The geometric figure of the whole mount is also called tetrahedron. When lead screw AD becomes longer, the antenna will rotate around axis MB; when BC becomes longer the axis will be MD. Hence the hinge lines MB and MD are formed by two points, the foundation plane ABM and the reflector plane CDM by three points. All forces exerted on the reflector are guided directly to the concrete pedestal, therefore, if friction and backlash of this simple system are controlled, an adequate antenna mount is obtained.

It is an advantage that the construction is mounted on the ground with only three points so that remounting and readjusting to receive a different geostationary satellite is rather simple. However, it is a disadvantage that the axes are not orthogonal, therefore, a computer is needed to steer the antenna in azimuth and elevation.

4. Modification of the main pointing direction

In the previous section it is explained that the mount has a small range. But sometimes the antenna will have to be pointed from one geostationary satellite to another. However, all geostationary satellites are moving on a big circle with the equator. Almost from every position on earth, except north and south

pole, we can see a part of this big circle. At the ground station in Eindhoven ($51^{o}27'$ north latitude and $5^{o}30'$ east longitude) the equatorial orbit of all geostationary satellites can easily be computed. To determine the position of the ATS 6 satellite first the azimuth has to be calculated by means of Fig. 7. In Fig. 7, Eindhoven is indicated by B, the satellite by C, the equator by AC and the meridian by AB.
Knowing the position of Eindhoven and also the subsatellite point, the azimuth angle ϕ is easily to compute using spherical trigonometry. The position of Eindhoven is:

$$51^{o}27' \text{ north latitude} = \text{arc } AB$$
$$5^{o}30' \text{ east longitude} = \text{arc } AD$$

The position of the subsatellite point is 0^{o} north latitude .

$$35^{o} \text{ east longitude} = \text{arc } DC$$

further

$$\text{arc } AC = 29^{o}30'$$

and

$$\text{angle } BAC = 90^{o}.$$

The first cosine equation in triangle BAC now gives:

$$\cos BC = \cos AC \cos AB + \sin AC \sin AB \cos BAC$$
$$\cos BC = \cos AC \cos AB + 0$$
$$\cos BC = 0.5424 \rightarrow BC = 57^{o}9'$$

Using the cosine equation again we obtain but now for Δ ABC

$$\cos AC = \cos BC \cos AB + \sin BC \sin AB \cos \phi$$

$$\cos \phi = \frac{\cos AC - \cos BC \cos AB}{\sin BC \sin AB}$$

$$\cos \phi = 0.8102, \text{ thus the azimuth angle } \phi = 35.88.$$

To calculate the elevation angle ψ, we draw a cross section over the earth, showing Eindhoven, the middle of the earth and the satellite (Fig. 8). Using

plane geometry we can calculate the elevation angle ψ as follows:
In triangle MBS the cosine equation results in

$$BS^2 = MB^2 + MS^2 - 2MB.MS.\cos 57^\circ 9'$$

and $MS^2 = MB^2 + BS^2 - 2MB.BS.\cos(90^\circ + \psi)$,

where

$$\cos(90^\circ + \psi) = \frac{-MS^2 + MB^2 + BS^2}{2MB.BS} = -0.422,$$

or $\cos(90^\circ + \psi) = -\sin\psi$, thus the elevation ψ = 24.99 degrees.

A similar azimuth elevation calculation can be made up for any geostationary satellite seen from Eindhoven as shown below. Let us suppose that the sub-satellite point on the equator has a certain position east longitude which we will call EL degrees.

Then arc AC = EL - $5^\circ 30'$.

Using the first cosine equation in triangle BAC we obtain results similar as before:

$$\cos BC = \cos AC \cos AB$$

or $\cos BC = \cos (EL - 5^\circ 30') \cos 51^\circ 27'$.

Using the cosine equation again gives:

$$\cos \phi = \frac{\sin 51^\circ 27' \cos (EL - 5^\circ 30')}{\sqrt{1 - \cos^2 51^\circ 27' \cos^2(EL - 5^\circ 30')}}$$

or simpler, using decimal degrees:

$$\text{azimuth } \phi = \arccos \frac{0.782065 \cos (EL - 5.5)}{\sqrt{1-0.388375 \cos^2(EL-5.5)}}$$

A general equation giving the elevation at Eindhoven can also be found (Fig. 8).
The cosine equation in triangle MBS (decimal degrees again) gives:

$$BS^2 = MB^2 + MS^2 - 2MB.MS.\cos BC$$

or $BS^2 = MB^2 + MS^2 - 2MB.MS.\cos (EL - 5.5) \cos 51.45$.

Further:

$$MS^2 = MB^2 + BS^2 - 2MB.BS.\cos(90 + \psi)$$

or $$\cos (90 + \psi) = \frac{-MS^2 + MB^2 + BS^2}{2\ MB.BS}$$

or $$\cos (90 + \psi) = - \sin \psi = \frac{MB - MS \cos (EL - 5.5) \cos 51.45}{BS},$$

$$\text{elevation } \psi = \arcsin \frac{26.29 \cos (EL - 5.5) - 6.37}{\sqrt{1819.73 - 333.89 \cos (EL-5.5)}}$$

Calculating more of these points give enough data to construct the equatorial orbit as seen from Eindhoven (Fig. 9). The ATS-6 satellite is seen from Eindhoven at 35.88 degrees azimuth and 24.99 degrees elevation. Naturally, we also can indicate the azimuth angle from the north. In that case the azimuth angle would be 144.12 degrees. If the antenna, in a position to receive ATS-6, needs to point to a different geostationary satellite, the antenna pointing axis will have to move along the arc shown in Fig. 9. It can be realised by turning the whole mount around a polar axis, being an axis parallel to the axis of the earth. The Eindhoven mount is provided with such a polar axis. Two of the three frame points A and B of Fig. 6 are situated on a curved rail parallel with the equator. Remounting A and B on a different spot means rotating around that polar axis and thus scanning the equatorial orbit. We indicate the rotating around the polar axis by angle β. If $\beta = 0$ the antenna is pointing southwards; if β is positive the antenna looking eastwards and if β is negative the antenna looks to the west. Fig. 10 shows the Eindhoven antenna mount, the construction of Fig. 5 is easily recognised. The lead screws AD and BC are clearly noticed. Rotating around the polar axis only means displacing A and B, viz. A becomes to A* and B becomes B*. The constant parameters of the system are the angles ε and β. The angle β indicates the rotation around the polar axis and ε is a constant elevation angle in the frame work. These parameters are connected with the location of satellite and ground station. The variable parameters are the lengths of the two lead screws. The maximum variation of these parameters gives the antenna range.
The position of the OTS satellite is 10° East. From the above it follows that at Eindhoven the satellite is seen azimuth = 5.7° East and the elevation 30.9°. The position of the SIRIO satellite is 15° West, then azimuth is $25^{\circ}12'$ West and elevation $28^{\circ}48'$.

5. The coordinate transformation

All system lengths of the mount are equal: this means that A, B, C and D all have the same distance to point M and further that AB, BD and CD are also equal (Fig. 10). In this way a sphere is formed with centre M and the points A, B, C and D on the surface (Fig. 11).
Because the three points C, D and M form the reflector plane, this plane is seen

as a circle on the sphere mentioned above. On this sphere also a horizontal circle may be drawn. On this horizontal circle, north, south, east and west can be indicated. Because both circles, reflector circle and horizontal circle, have M for centre they intersect each other. Using the parameters ϕ and ξ, the position of the reflector plane in relation to the horizontal plane can be described. The angle ξ between both planes indicates the elevation, ϕ is the arc between the reference east and the point of intersection of both circles and indicates the direction in which the antenna is pointing (azimuth). To obtain a relation between the two circles, the points A, B, C, D and point P where the polar axis intersects the surface of the sphere are drawn in Fig. 12. The north of the horizontal circle is called R. The arc RP is 52 degrees. Because in the antenna construction A and B are situated on a circle around the polar axis the distance AP is equal to BP. If the antenna is pointing southwards, A and B are symmetrical to the line PR, point N lies on PR and arc NR is equal to ε (Fig. 10). Thus PN is (52-ε) degrees.

In Fig. 12 the antenna is not pointing southwards, but rotated over an angle β around the polar axis. Therefore, the points A, B, C and D are displaced. Because the lengths AB, BD and CD are equal to the radius of the sphere, the arcs AB, BD and CD are all 60 degrees. AN = BN = 30^{o}. Arc K and arc L belong to the right and left lead screw.

In appendix I the parameter ξ, indicating elevation, is expressed in the variables ε, β, arc L and arc K. The parameters ε and β have a permanent character and can be fixed, ε is 17 degrees and when the antenna is pointing to ATS-6, β amounts 27 degrees.

With fixed ε and β the azimuth ϕ and elevation ψ of the antenna are easy to find. In Fig. 13 we see the relation between the angle ξ and the elevation angle ψ: $\psi = 90^{o} - \xi$, thus $\sin\psi = \cos\xi$.

The azimuth can be found as follows: point R in Fig. 12 indicates precisely the north. As QR amounts 90 degrees, the antenna is pointing southwards. When QR < 90 degrees the antenna is rotated ϕ degrees to the east. $\phi = 90^{o} - QR$ (Fig. 13). The second cosine equation applied in Δ QRZ gives QR:

$$\cos\xi = -\cos\xi\cos\rho + \sin\xi\sin\rho\cos QR$$

$$\rho = 90^{o} \rightarrow \cos\zeta = \sin\xi\cos QR \qquad \cos QR = \frac{\cos\xi}{\sin\xi}\ .$$

The screw actuators K and L vary between 80 and 100 centimetres. All other system lengths are 133 centimetres.

In this way the minimum and maximum value of arc L and K may be calculated (Fig. 15).

Kmax = Lmax = 100 cm.

arc Kmax = 2μ; $\mu = \arcsin \frac{50}{133} \rightarrow \mu = 22.08^{o}$.

Thus: arc Lmax = arc Kmax = 44.1648^{o}

arc Lmin = arc Kmin = 35.0055^{o}.

After substitution these values in the coordinate transformation we find:

$\beta = 27^{o}$ $\varepsilon = 17^{o}$

Kmax, Lmax	ϕ = 36,53 degrees; ψ = 20,83 degrees	Lmin, Kmin	ϕ = 36,01 degrees; ψ = 29,25 degrees
Lmax, Kmin	ϕ = 26,43 degrees; ψ = 26,44 degrees	Lmin, Kmax	ϕ = 44,97 degrees; ψ = 22,05 degrees

$\beta = 0$ $\varepsilon = 17^{o}$

Lmax, Kmax	ϕ = 8,25 degrees; ψ = 27,17 degrees	Lmin, Kmin	ϕ = 4,77 degrees; ψ = 35,07 degrees
Lmax, Kmin	ϕ = -3,71 degrees; ψ = 29,72 degrees	Lmin, Kmax	ϕ = 16,47 degrees; ψ = 30,55 degrees

It is significant that when $\beta = 0$ the antenna is not exactly pointing southwards. The reason is the asymmetry of the antenna configuration. The diagonal rotates the antenna a little to the east.

Fig. 16 shows a picture of the sky looking southwards. The antenna describes a diamond shaped figure of about 10 degrees elevation and 20 degrees azimuth. The ATS-6 track is drawn as a little dash at $\phi = 36^{o}$ and $\psi = 25^{o}$.

Photograph 3 shows the entire steering mechanism and also the curved mounting rail.

6. The ideal mount

The mount has some disadvantages. First the axes are not orthogonal, a very complex coordinate transformation being the result. Second the polarisation has to be adjusted continuously.

The reason is that the concept of the mount was only made for following a satellite in the two dimensional azimuth-elevation space. Therefore, two degrees of freedom were built in, guided by two stepping motors. Afterwards the third degree of freedom, the polarisation adjustment provision, was needed.

This would not have been necessary, if the main axis of the mount was directed parallel to the polarisation direction. As the signal is polarised linear north-south a polar axis would be desirable. This means an axis parallel to the axis of the earth. Further it is difficult to measure the radiation pattern of the antenna because rotation of the antenna to the desired direction must be carried out by steering the two stepping motors at the same time. It would be ideal if the two axes of the mount were parallel with the copolar and cross-polar direction in the aperture plane. In that case only one single stepping motor would be needed to measure the radiation pattern.

It is possible to avoid these disadvantages. In Fig. 17 the first drawing shows the mount suggested in Fig. 6 being the actual mount located in Eindhoven. The mean axis, connected to the earth, is MA. Displacing the entire mount will make MA a polar axis. This is shown in Fig. 17.2.

To obtain an orthogonal mount the second axis MC has to be perpendicular to the main axis MA. Therefore, the length of bar AC has to be changed, shown in Fig. 17.3. This picture shows the ideal mount: the main axis MA is parallel to the axis of the earth, the second axis MC is perpendicular to the main axis giving an orthogonal system. Elongation of screw actuator AD gives a rotation around axis MC and elongation of lead screw BC gives a rotation around MA.

This means that there is one stepping motor for rotation around each axis; the MA axis is identical with the copolar direction and the MC axis is identical with the cross polar direction. This means that no third degree of freedom, rotating the feed horn, is needed. Moving the lead screws separately is sufficient. This mount has global coordinates so that tracking is possible knowing the global position of the satellite.

Further the small range of the antenna would fit very well the equatorial orbit. The rims of the reach are parallel and perpendicular to the orbit as is shown in Fig. 18.

Displacing the reach would be possible by remounting point B in Fig. 17.3 on a circle around the polar line AM.

7. Specifications and technical data

1. Drive

Antenna positioning by means of two lead screws. These are driven by stepping motors of manufacture: Superior Electric; type HS 50 L-1011; 200 steps per revolution. Torque: 21.6 kg.cm. at 150 steps per second.

2. Position indication

Position indication by means of absolute encoders of manufacture: Moor Reed, type 23 DD 167 with a range of 50 turns; 400 steps per revolution. These encoders are connected to the lead screws. The score is shown by a LED display on the control board. The transmission provides that the total acting lead screw length is proportional to one complete encoder reach.

3. Manual operation

Number of steps adjustable between -9999 and +9999 by means of 5 thumb wheel switches per motor. Positioning begins after pressing the "start" button that switches both stepping motors.

4. Tracking

Program tracking by means of Tally PR 2000 - tape reader

- Number of steps per motor 0 until 9999 (ASCII-code)
- Direction A (reverse) or V (ahead) (ASCII-code)
- Positioning begins automatically by a start command at the end of the read-in cycle
- Read-in velocity is limited by a tape reader and amounts maximally 300 signs per second
- Time interval between read-in-cycles adjustable on 1, 2, 5, 10 or 20 minutes (derived from power supply frequency).

5. Lead screws

Specifications of the lead screw construction:

1. The steering system is accurate up to wind velocities of about 20 metres per second. The entire construction has proved to be resistent against heavy storm.
2. Accuracy.
   One revolution of the stepping motor gives 1 millimetre displacement of the lead screw. At the fixed size of the system this is proportional to a rotation of about 0.05 degrees. This is subdivided into 200 steps. Hysteresis amounts 0.002 degrees.
3. Read out accuracy is also 0.002 degrees.
4. Total range: elevation ~ 10 degrees   azimuth ~ 20 degrees (Fig. 11).

5. Velocity for the entire range of one lead screw: 4.5 minutes.

6. General

The steering electronics mostly consists of C-Mos digital integrated circuits; Manufacture: National Semiconductor. On locations where larger currents are required (motor drive, LED-drivers) Teledyne HiNiL has been used. The input and output circuits regarding the tape readers and computer steering, are provided with level adaptation: TTL - C - Mos and reverse.
The antenna mount consists of three parts:

1. A concrete pedestal and attached to it a circular mounting rail and a mounting plate for a ball hinge.
   In other constructions also a simpler pedestal could be made by simple little walls. This is probably cheeper and more suitable for roof mounting. The pedestal has to be lined out in the direction North-South.
2. The two lead screws construction and five ball hinges. All have an anti-backlash provision.
3. A triangular subframe for mounting the parabolic reflector. It will be possible to turn and exchange reflectors in one hour and with some adaption more types of reflectors are applicable. Reflector diameter about 3 metres.

Acknowledgement

The authors wish to express their gratitude to Prof. W. van den Hoek for his valuable suggestions and discussions related to this subject.

References

1. Jakes, W.C.: "Participation of Bell Telephone Laboratories in project ECHO and experimental results",
   Bell Syst. Techn. J., Vol. 40, nr. 4, pp. 975-1028, July 1961.

2. Filipowsky R.F. and Muehldorf E.I.: "Space communication systems",
   Prentice Hall Inc., Englewood Cliffs, N.J., U.S.A. 1965.

3. Martin E.J.: "Commercial satellite communication experience",
   IEEE Northeast Electronics Research and Engineering Meeting NEREM,
   pp. 105-105, Boston 1966.

4. Silver, S.: "Microwave antenna theory and design",
New York, Mc Graw Hill, 1949.

Appendix I Transformation calculations

Here the parameter ξ, indicating the elevation, will be expressed in the variables ε, β, arc L and arc K. Therefore, we apply some simple equations from the spherical and plane trigonometry such as:

Spherical trigonometry

first cosine equation: $\cos a = \cos b \cos c + \sin b \sin c \cos \alpha$

second cosine equation: $\cos \alpha = -\cos \beta \cos \gamma + \sin \beta \sin \gamma \cos a$

sin equation: $\frac{\sin a}{\sin \alpha} = \frac{\sin b}{\sin \beta} = \frac{\sin c}{\sin \gamma}$

General trigonometry equations:

$\sin(\alpha \pm \beta) = \sin\alpha \cos\beta \pm \cos\alpha \sin\beta$

$\cos(\alpha \pm \beta) = \cos\alpha \cos\beta \pm \sin\alpha \sin\beta$

Known $PR = 52^o$

$AB = BD = CD = 60^o$

$PN = 52^o - \varepsilon$

$AN = NB = 30^o$

In triangle NPT (Fig. 12) the second cosine equation gives:

$$\cos\chi = -\cos\beta \cos\nu + \sin\beta \sin\nu \cos PN$$

$$\cos\chi = -\cos\beta \; 0 + \sin\beta \; .1. \cos(52-\varepsilon) \quad (1)$$

$$\underline{\cos\chi} = \sin\beta \cos(52-\varepsilon)$$

$$(1) \rightarrow \underline{\sin\chi} = \sqrt{1-\cos^2\chi} = \sqrt{1-\sin^2\beta \cos^2(52-\varepsilon)} \quad (2)$$

Second cosine equation in triangle NPT:

$$\cos\nu = -\cos\chi \cos\beta + \sin\chi \sin\beta \cos PT$$

$$\cos PT = \frac{\cos\chi \cos\beta}{\sin\chi \sin\beta} = \frac{\cos(52-\varepsilon) \sin\beta \cos\beta}{\sin\beta \sqrt{1-\sin^2\beta \cos^2(52-\varepsilon)}}$$

$$\underline{\cos PT} = \frac{\cos(52-\varepsilon) \cos\beta}{\sqrt{1-\sin^2\beta \cos^2(52-\varepsilon)}} \quad (3)$$

$$\underline{\sin PT} = \sqrt{1-\cos^2 PT} = \frac{\sin(52-\varepsilon)}{\sqrt{1-\sin^2\beta \cos^2(52-\varepsilon)}} \quad (4)$$

$TR = PR - PT = 52^{o} - PT$

$\sin TR = \sin(52^{o} - PT) = \sin 52 \cos PT - \cos 52 . \sin PT$

$$\sin TR = \frac{\sin 52^{o} \cos\beta . \cos(52-\varepsilon)}{\sqrt{1 - \sin^2\beta \cos^2(52-\varepsilon)}} - \frac{\cos 52 \sin(52-\varepsilon)}{\sqrt{1-\sin^2\beta \cos^2(52-\varepsilon)}}$$

$$\underline{\sin TR} = \frac{\sin 52^{o} \cos\beta \cos(52-\varepsilon) - \cos 52^{o} \sin(52-\varepsilon)}{\sqrt{1-\sin^2\beta \cos^2(52-\varepsilon)}} \tag{5}$$

check: if $\beta = 0 \rightarrow TR = \sin \varepsilon$.

$\cos.(PR-PT) = \cos 52^{o} \cos PT + \sin 52^{o} \sin PT$

$$\underline{\cos TR} = \frac{\cos 52^{o} \cos(52-\varepsilon) . \cos\beta + \sin 52 \sin(52-\varepsilon)}{\sqrt{1 - \sin^2\beta \cos^2(52-\varepsilon)}} \tag{6}$$

In Δ NPT second cosine equation:

$\cos.\beta = -\cos\chi \cos\nu + \sin\chi \sin\nu \cos TN$

$$\underline{\cos TN} = \frac{\cos\beta}{\sin\chi} = \frac{\cos\beta}{\sqrt{1 - \sin^2\beta \cos^2(52-\varepsilon)}} \tag{7}$$

$$\sin TN = \sqrt{1 - \cos^2 TN} = \sqrt{\frac{1 - \sin^2\beta \cos^2(52-\varepsilon)}{1 - \sin^2\beta \cos^2(52-\varepsilon)} - \frac{\cos^2\beta}{1 - \sin^2\beta \cos^2(52-\varepsilon)}}$$

$$\sin TN = \sqrt{\frac{\sin^2\beta + \cos^2\beta - \sin^2\beta \cos^2(52-\varepsilon) - \cos^2\beta}{1 - \sin^2\beta \cos^2(52-\varepsilon)}} = \frac{\sin\beta \sqrt{1 - \cos^2(52-\varepsilon)}}{\sqrt{1 - \sin^2\beta \cos^2(52-\varepsilon)}}$$

$$\underline{\sin TN} = \frac{\sin\beta . \sin(52-\varepsilon)}{\sqrt{1 - \sin^2\beta \cos^2(52-\varepsilon)}} \tag{8}$$

$\sin TB = \sin(TN+NB) = \sin TN \cos 30^{o} + \cos TN . \sin 30^{o}$.

$$\sin TB = \frac{\sqrt{3} \sin\beta . \sin(52-\varepsilon)}{2 . \sqrt{1 - \sin^2\beta \cos^2(52-\varepsilon)}} + \frac{\cos\beta}{2\sqrt{1 - \sin^2\beta . \cos^2(52-\varepsilon)}}$$

$$\sin TB = \frac{\sqrt{3} \sin\beta \sin(52-\varepsilon) + \cos\beta}{2\sqrt{1 - \sin^2\beta \cos^2(52-\varepsilon)}} \tag{9}$$

$\cos TB = \cos(TN+NB) = \cos TN . \cos 30^{o} - \sin TN \sin 30^{o}$.

$$\cos TB = \frac{\sqrt{3} \cos \beta}{2\sqrt{1 - \sin^2\beta \cos^2(52-\varepsilon)}} - \frac{\sin\beta . \sin(52-\varepsilon)}{2 . \sqrt{1 - \sin^2\beta \cos^2(52-\varepsilon)}}$$

$$\underline{\cos TB} = \frac{\sqrt{3} \cos\beta - \sin\beta . \sin(52-\varepsilon)}{2\sqrt{1 - \sin^2\beta \cos^2(52-\varepsilon)}} \tag{10}$$

First cosine equation in Δ ABD gives

$$\cos L = \cos DB . \cos AB + \sin DB . \sin AB \cos\lambda$$

$$\cos L = \cos 60^\circ . \cos 60^\circ + \sin 60^\circ \sin 60^\circ . \cos\lambda$$

$$\cos\lambda = \frac{\cos L - \cos^2 60}{\sin^2 60} = \frac{4}{3} (\cos L - \frac{1}{4}) = \frac{1}{3} (4\cos L - 1) \qquad (11)$$

$$\sin\lambda = \sqrt{1-\cos^2\lambda} = \frac{\sqrt{9-(4\cos\lambda-1)^2}}{3} \qquad (12)$$

This is also valid in Δ BCD.

So:

$$\underline{\cos\lambda} = \frac{4}{3} \cos L - \frac{1}{3} \quad (11) \qquad \underline{\sin\lambda} = \frac{1}{3}\sqrt{9-(4\cos L-1)^2} \qquad (13)$$

$$\underline{\cos K} = \frac{4}{3} \cos K - \frac{1}{3} \quad (13) \qquad \underline{\sin K} = \frac{1}{3}\sqrt{9-(4\cos K-1)^2} \qquad (14)$$

In Δ TBS the second cosine equation yields

$$\cos\sigma = - \cos\lambda \cos\chi + \sin\lambda \sin\chi \cos TB$$

$$\underline{\cos\sigma} = - \frac{1}{3}(4\cos L-1)(\sin\beta\cos(52-\varepsilon) + \frac{1}{3}\sqrt{9-(4\cos L-1)^2}\ \frac{\sqrt{3}\cos\beta-\sin\beta\sin(52-\varepsilon)}{2} \qquad (15)$$

$$\underline{\sin\sigma} = \sqrt{1 - \cos^2\sigma} \qquad (16)$$

The sine equation in Δ TBS results in:

$$\frac{\sin ST}{\sin \lambda} = \frac{\sin TB}{\sin\sigma} \qquad \sin ST = \frac{\sin TB \sin\lambda}{\sin\sigma}$$

$$\underline{\sin ST} = \frac{(\sqrt{3} \sin\beta \sin(52-\varepsilon) + \cos\beta)\ \frac{1}{3}\sqrt{9-(4\cos L-1)^2}}{2 \sin\sigma\sqrt{1-\sin^2 \beta\cos^2(52-\varepsilon)}} \qquad (17)$$

and the second cosine equation:

$$\cos\lambda = -\cos\sigma \cos\chi + \sin\sigma \sin\chi \cos ST$$

$$\cos ST = \frac{\cos\lambda + \cos\sigma \cos\chi}{\sin\sigma \sin\chi}$$

$$\cos ST = \frac{\frac{1}{3} (4\cos L-1) + \cos\sigma \sin\beta \cos(52-\varepsilon)}{\sin\sigma \sqrt{1-\sin^2\beta \cos^2(52-\varepsilon)}} \qquad (18)$$

In Δ BST the sine equation yields

$$\frac{\sin TS}{\sin\lambda} = \frac{\sin BS}{\sin\chi} \rightarrow \sin BS = \frac{\sin TS \sin\chi}{\sin\lambda}$$

$$\sin BS = \frac{(\sqrt{3}\sin\beta\sin(52-\varepsilon) + \cos\beta)\frac{1}{3}\sqrt{9-(4\cos L-1)^2}}{2\sin\sigma\sqrt{1-\sin^2\beta\cos^2(52-\varepsilon)}} \cdot \frac{\sqrt{1-\sin^2\beta\cos^2(52-\varepsilon)}}{\frac{1}{3}\sqrt{9-(4\cos L-1)^2}}$$

$$\sin BS = \frac{\sqrt{3}\sin\beta\sin(52-\varepsilon) + \cos\beta}{2\sin\sigma} \qquad (19)$$

and the second cosine equation:

$$\cos\chi = -\cos\lambda\cos\sigma + \sin\lambda\sin\sigma\cos BS$$

$$\cos BS = \frac{\cos\chi + \cos\lambda\cos\sigma}{\sin\lambda\sin\sigma}$$

$$\underline{\cos BS} = \frac{\sin\beta\cos(52-\varepsilon) + \frac{1}{3}(4\cos L-1)\cos\sigma}{\frac{1}{3}\sqrt{9-(4\cos L-1)^2}\sin\sigma} \qquad (20)$$

$$\sin SD = \sin(BD-BS) = \sin(60^\circ-BS) = \sin 60^\circ\cos BS - \cos 60\sin BS$$

$$\sin SD = \frac{1}{2}\sqrt{3}\cos BS - \frac{1}{2}\sin BS$$

$$\underline{\sin SD} = \frac{\sqrt{3}\sin\beta\cos(52-\varepsilon) + \frac{1}{3}\sqrt{3}(4\cos L-1)\cos\sigma}{2/3\sqrt{9-(4\cos L-1)^2}.\sin\sigma} - \frac{\sqrt{3}\sin\beta\sin(52-\varepsilon)+\cos\beta}{4\sin\sigma} \qquad (21)$$

$$\cos SD = \cos(60^\circ-BS) = \cos 60\cos BS + \sin 60\sin BS$$

$$\cos SD = \frac{1}{2}\cos BS + \frac{1}{2}\sqrt{3}\sin BS$$

$$\underline{\cos SD} = \frac{3\sin\beta\cos(52-\varepsilon) + (4\cos L-1)\cos\sigma}{2\sqrt{9-(4\cos L-1)^2}\sin\sigma} + \frac{3\sin\beta\sin(52-\varepsilon) + \sqrt{3}\cos\beta}{4\sin\sigma} \qquad (22)$$

The second cosine equation applied in Δ SDZ gives:

$$\underline{\cos\zeta} = -\cos\sigma\cos K + \sin\sigma\sin K\cos SD \qquad (23)$$

$$\sin\zeta = \sqrt{1-\cos^2\zeta} \qquad (24)$$

and the sine equation in Δ SDZ:

$$\frac{\sin SD}{\sin\zeta} = \frac{\sin SZ}{\sin K}$$

$$\sin SZ = \frac{\sin SD . \sin K}{\sin\zeta}$$

$$\cos SZ = \sqrt{1-\sin^2 SZ} = \sqrt{1 \frac{\sin^2 SD \sin^2 K}{\sin^2\zeta}}$$

$$\sin RS = \sin(RT+TS) = \sin RT \cos TS + \cos RT \sin TS$$

$$\cos RS = \cos(RT+TS) = \cos RT \cos TS - \sin RT \sin TS$$

$$\cos RZ = \cos(RS+SZ) = \cos RS \cos SZ - \sin RS \sin SZ$$

$$\underline{\cos RZ} = \cos RT \cos TS \cos SZ - \sin TR \sin TS \cos SZ - \sin RT \cos TS \sin SZ - \cos RT \sin TS \sin SZ \quad (25)$$

Second cosine equation in Δ QRZ:

$$\cos\xi = -\cos\zeta \cos QRZ + \sin\zeta \sin QRZ \cos RZ$$

$$\text{angle } QRZ = 90^{\circ} \rightarrow \cos\xi = \sin\zeta \cos RZ$$

$$\cos\xi = (\cos RT \cos TS \cos SZ \sin\zeta) - (\sin RT \sin TS \cos SZ \sin\zeta) + -(\sin RT \cos TS \sin SZ \sin\zeta) - (\cos RT \sin TS \sin SZ \sin\zeta)$$

$$\underline{\cos\xi} = \text{term } 1 - \text{term } 2 - \text{term } 3 - \text{term } 4. \quad (26)$$

$$\text{term } 1 = \frac{\cos 52 \cos(52-\varepsilon) \cos\beta + \sin 52 \sin(52-\varepsilon)}{\sqrt{1 - \sin^2\beta \cos^2(52-\varepsilon)}} \times$$

$$\times \frac{\frac{1}{3}(4\cos L-1) + \cos\sigma \sin\beta \cos(52-\varepsilon)}{\sin\sigma \sqrt{1-\sin^2\beta \cos^2(52-\varepsilon)}} \times$$

$$\times \sqrt{\sin^2\zeta - \sin^2 SD \sin^2 K}.$$

$$\text{term } 2 = \frac{\sin 52 . \cos\beta . \cos(52-\varepsilon) - \cos 52 \sin(52-\varepsilon)}{\sqrt{1 - \sin^2\beta \cos^2(52-\varepsilon)}} \times$$

$$\times \frac{(\sqrt{3} \sin\beta \sin(52-\varepsilon) - \cos\beta) \frac{1}{3} \sqrt{9-(4\cos L-1)^2}}{2\sin\sigma \sqrt{1-\sin^2\beta \cos^2(52-\varepsilon)}} \times$$

$$\times \sqrt{\sin^2\zeta - \sin SD \sin^2 K}.$$

$$\text{term } 3 = \frac{\sin 52 \cos\beta \cos(52-\varepsilon) - \cos 52 \sin(52-\varepsilon)}{\sqrt{1 - \sin^2\beta \cos^2(52-\varepsilon)}} \times$$

$$\times \frac{\frac{1}{3} (4\cos L-1) + \cos\sigma \sin\beta \cos(52-\varepsilon)}{\sin\sigma \sqrt{1 - \sin^2\beta \cos^2(52-\varepsilon)}} \times \sin SD \sin K.$$

$$\text{term } 4 = \frac{\cos 52\ \cos(52-\varepsilon)\ \cos\beta + \sin 52\ \sin(52-\varepsilon)}{\sqrt{1 - \sin^2\beta\ \cos^2(52-\varepsilon)}} \times$$

$$\times \frac{(\sqrt{3}\ \sin\beta\ \sin(52-\varepsilon) + \cos\beta)\frac{1}{3}\ \sqrt{9-(4\cos L-1)^2}}{2\sin\sigma\ \sqrt{1-\sin^2\beta\ \cos^2(52-\varepsilon)}} \times \sin SD\ \sin K.$$

When we substitute in this long expression the equations for $\sin\sigma$ (15), $\sin\zeta$ (24) and $\sin K$ (14), then $\cos\xi$ is expressed in the parameters ε, β, K and L.

Appendix 2. Hysteresis measurements

The hysteresis of the pointing arrangement has been measured by means of an autocollimator and a mirror. These devices specially suitable for measuring very small angles very precisely.
A telescope and a collimator may be pointed to each other very precisely.
When the axes are not parallel a displacement "d" of the collimator mark over a distance of ϕ x f is visible (Fig. 19a).
For measuring only small angles the autocollimator is used which is a combination of a collimator and a telescope (Fig. 19.b). The cross mark is lightened for instance by means of a half reflecting little mirror and forms together with the objective a collimator. The measuring object is a mirror.
After reflection the cross is projected again in a cross and its location is measured. The inaccuracy can be reduced until 0.2 angular seconds; the measuring range is than small e.g. 10 angular minutes.
Because all the light beams between objective and mirror are parallel the distance between mirror and autocollimator is of no interest.
The hysteresis measured on the Eindhoven antenna amounts 0.5 . 10^{-3} vertical degrees and 2 . 10^{-3} horizontal degrees.

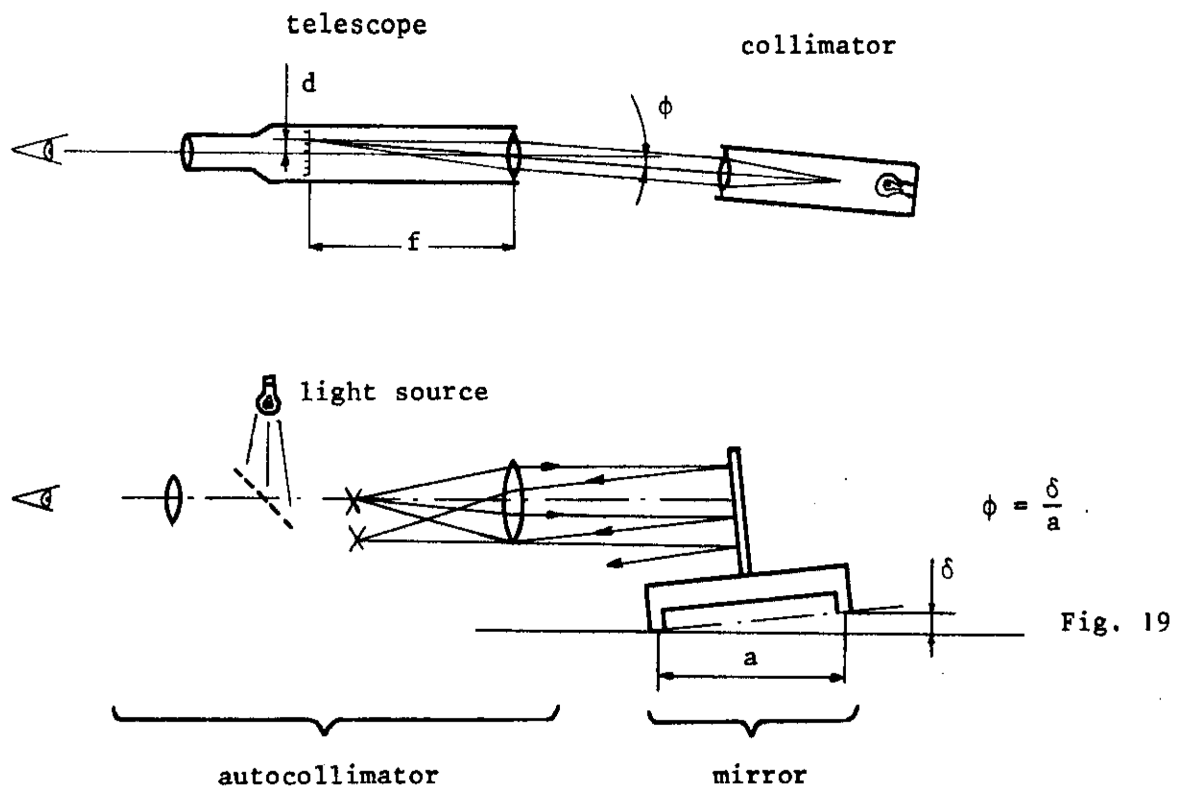

Fig. 19
a) Telescope and collimator. The distance between them is not important: d = f.ϕ
b) Autocollimator and mirror. The autocollimator combines a collimator and a telescope.

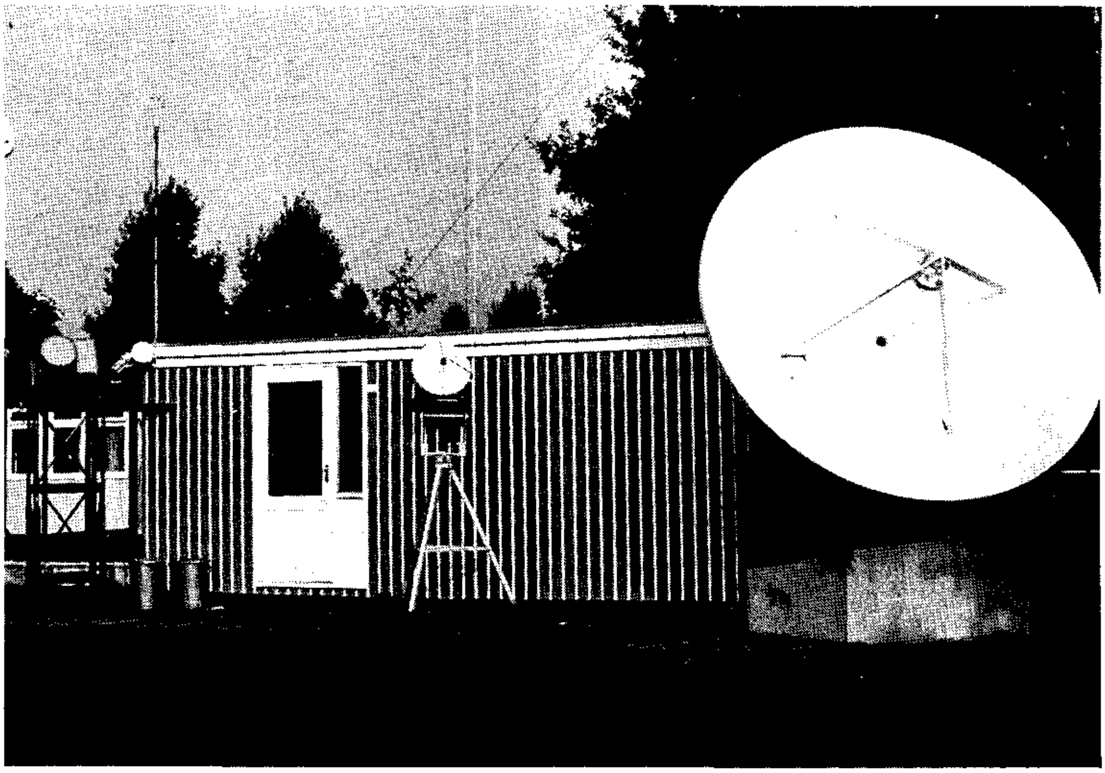

Photo 1 The 30 GHz Cassegrain antenna at Eindhoven University.

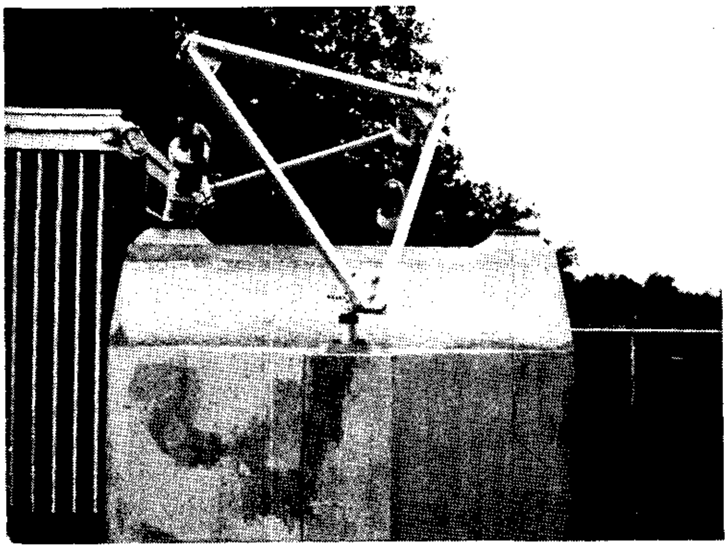

Photo 2 Mount without parabolic reflector. In front hinge M. Down at the lead screws, the points A and B disappear behind the concrete pedestal.

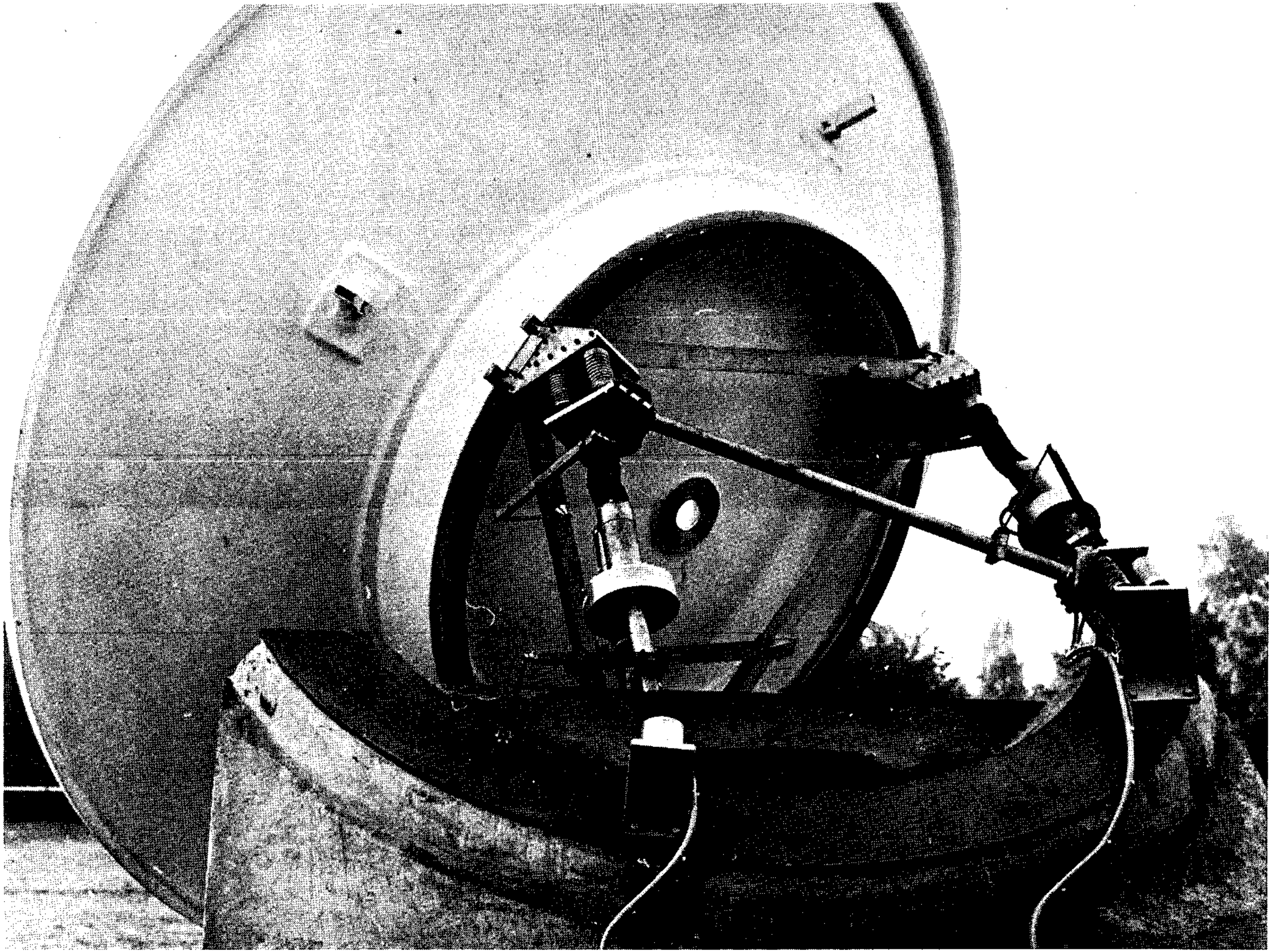

Photo 3 Back structure of the Eindhoven mount with two lead screws.

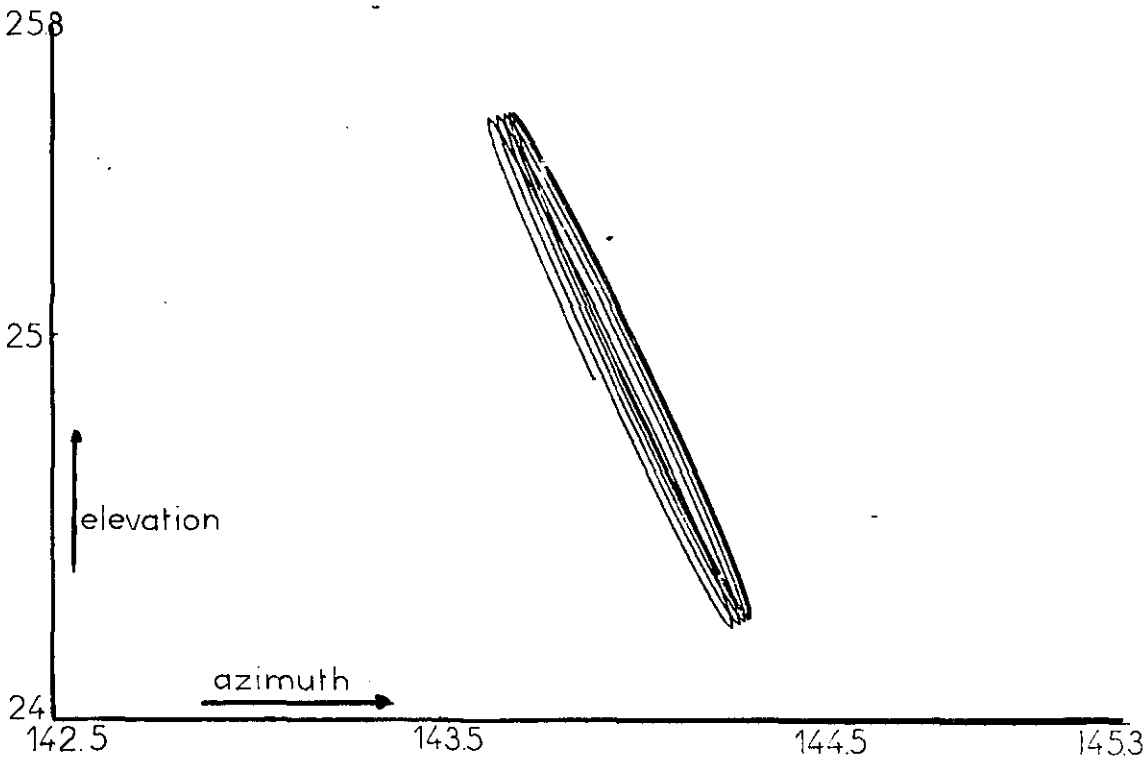

Fig. 1 ATS-6 satellite movements seen from Eindhoven

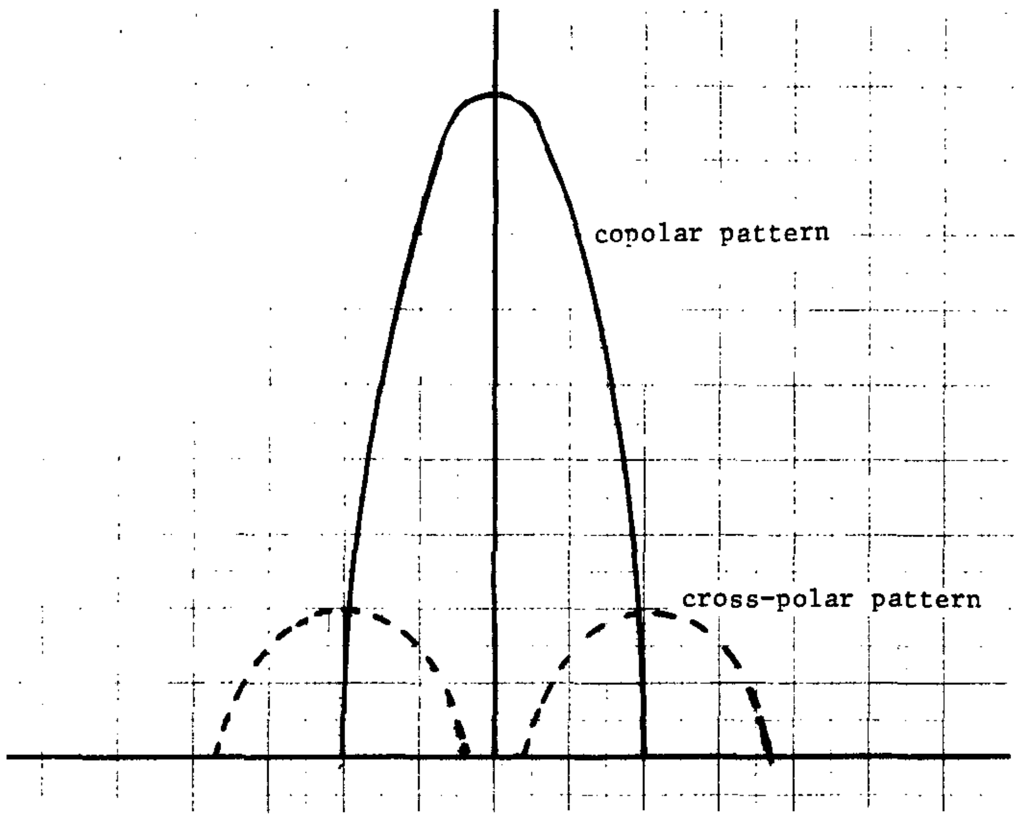

Fig. 2 The copolar and cross-polar radiation pattern of a reflector antenna

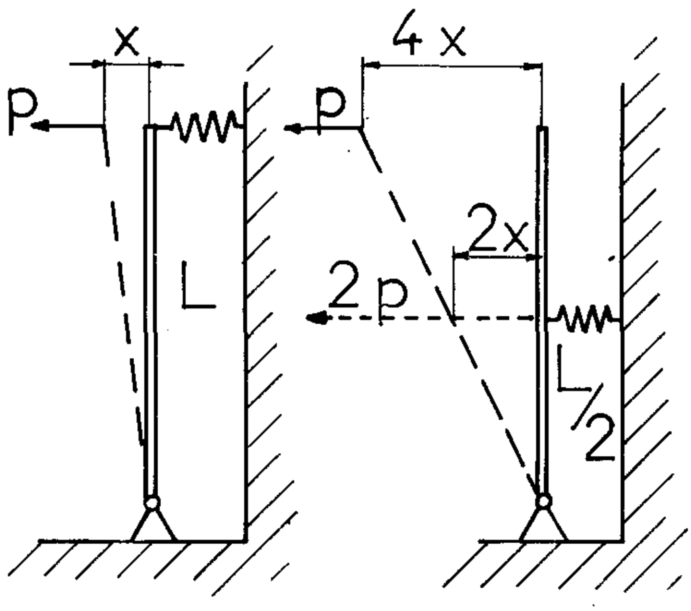

Fig. 3

a. Spring mounted at radius L
rigidity $c = \frac{P}{x}$

b. Spring mounted at radius L/2
rigidity $c = \frac{P}{4\ x}$

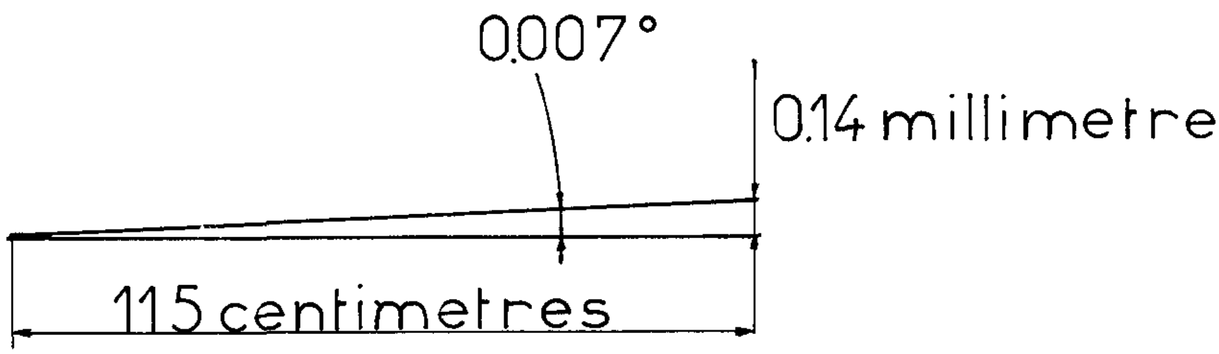

Fig. 4 Translation of 0.14 millimetres to an angle of 0.007 degrees

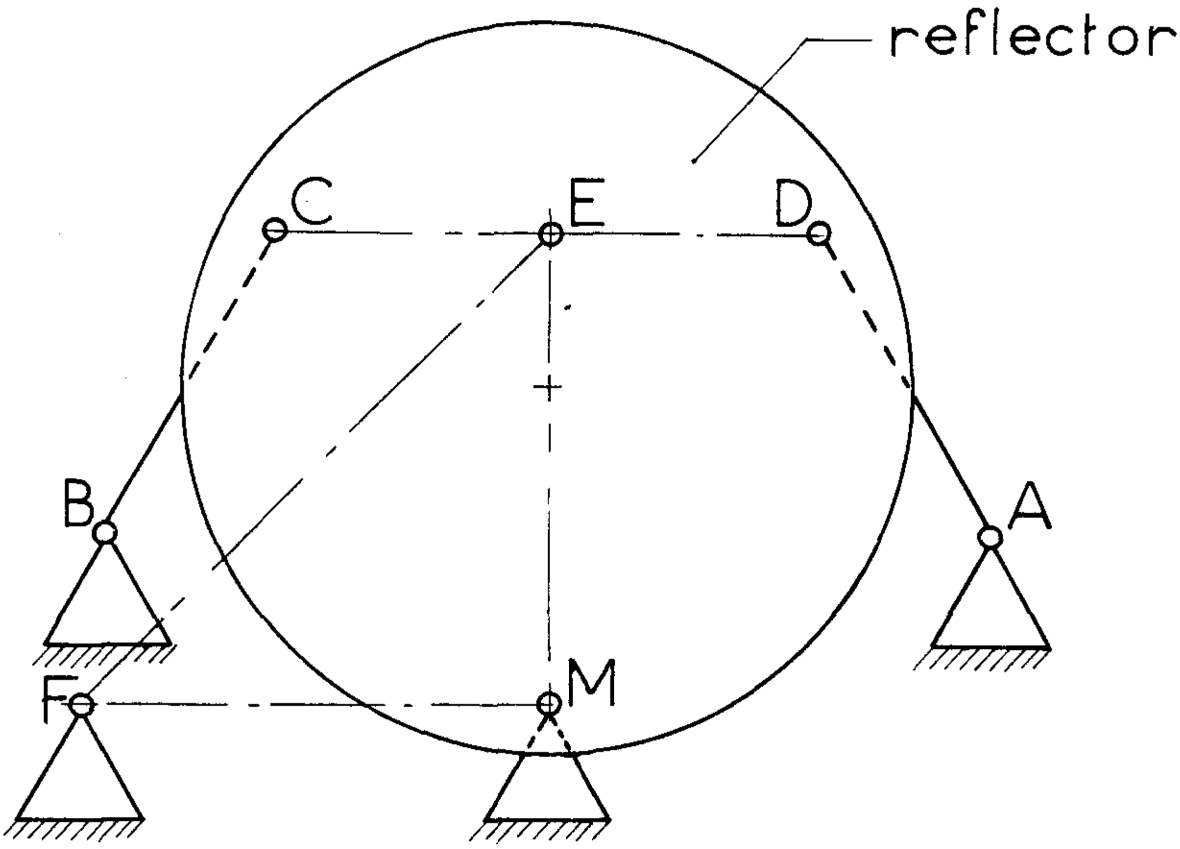

Fig. 5 Possible configuration of an antenna mount

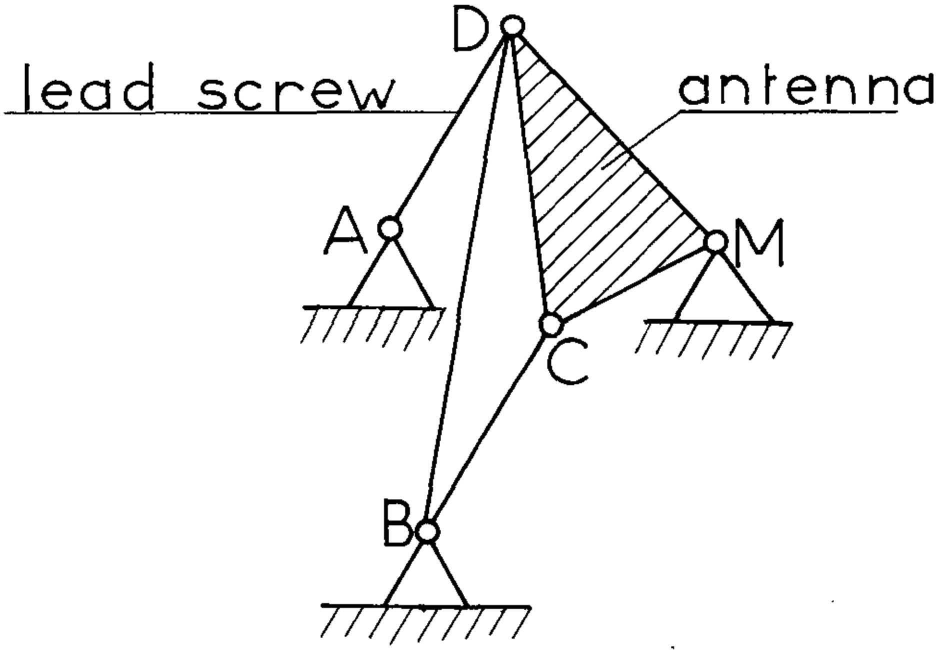

Fig. 6 Scetch of the kinematic construction of the antenna mount for ATS-6. AD and BC are the lead screws. AD growing longer forces the antenna to turn around axis BM. Elongation of BC generates a rotation of the antenna around DM.

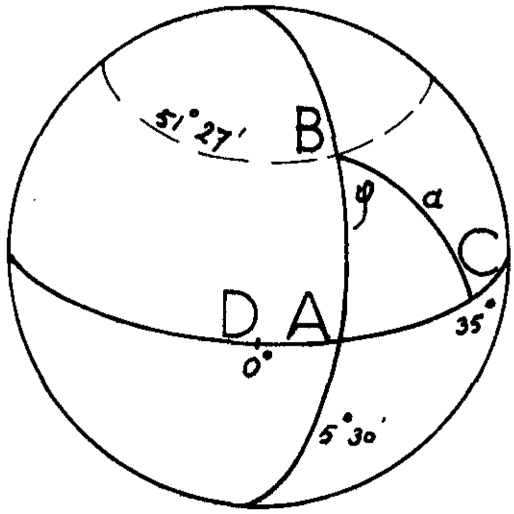

Fig. 7 The globe with Eindhoven (B), satellite point (C), equator AC and meridian AB. The azimuth angle at the Eindhoven ground station is called ϕ.

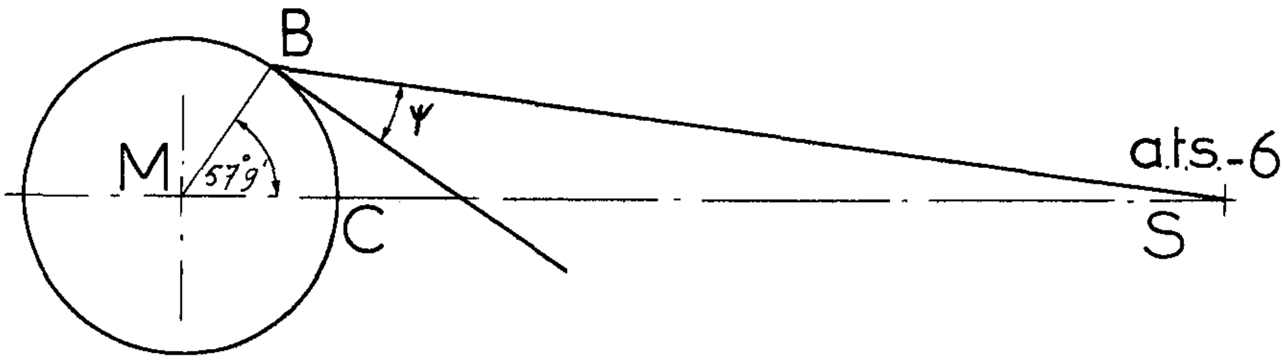

Fig. 8 Cross section through Eindhoven (B), middle of the earth M and satellite. North and south pole are not in this plane.

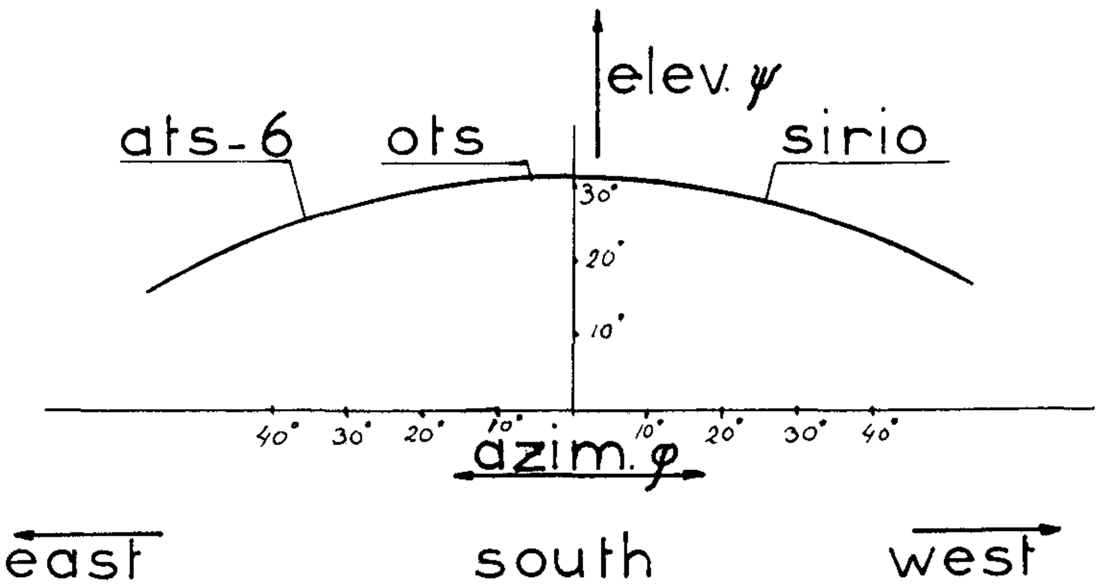

Fig. 9 Several geostationary satellites as seen from Eindhoven, looking southwards.

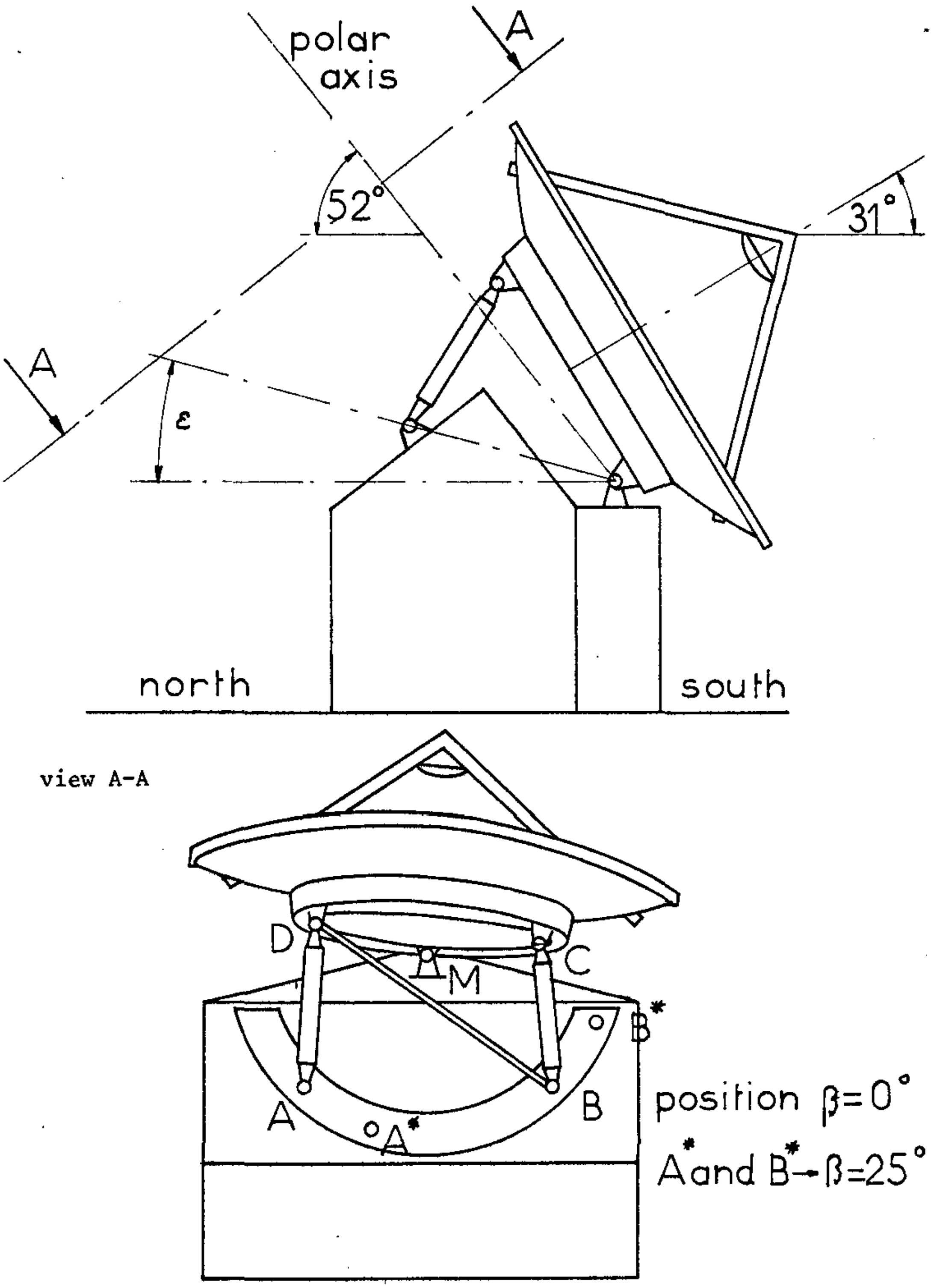

Fig. 10 The Eindhoven antenna pointing southwards; elevation 31 degrees; $\beta = 0$; $\varepsilon = 17^{o}$.

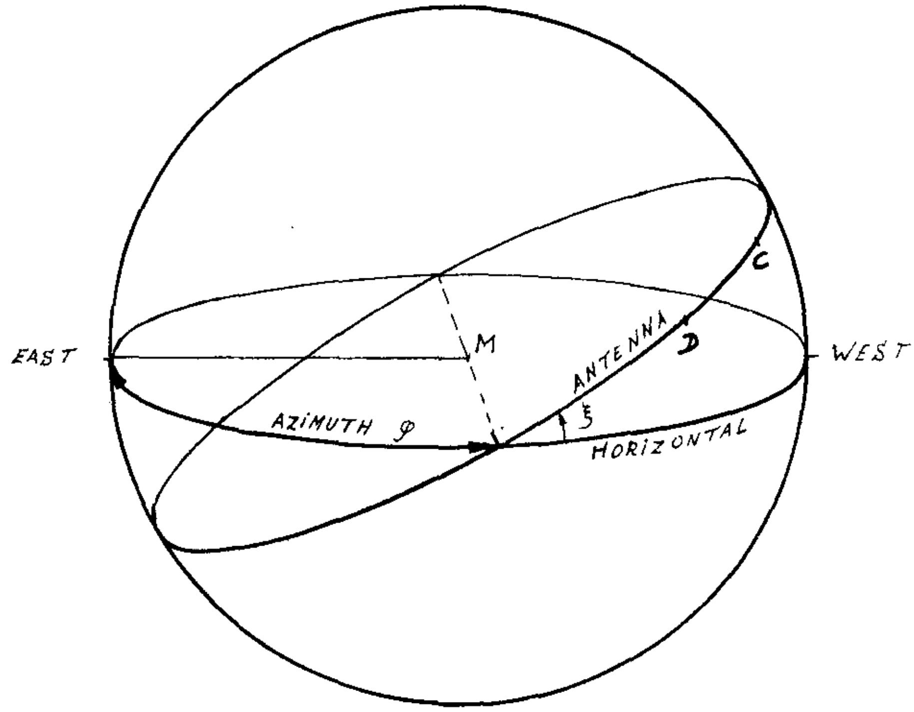

Fig. 11 The relation between the coordinates of the earth and azimuth and elevation of the reflector aperture plane.

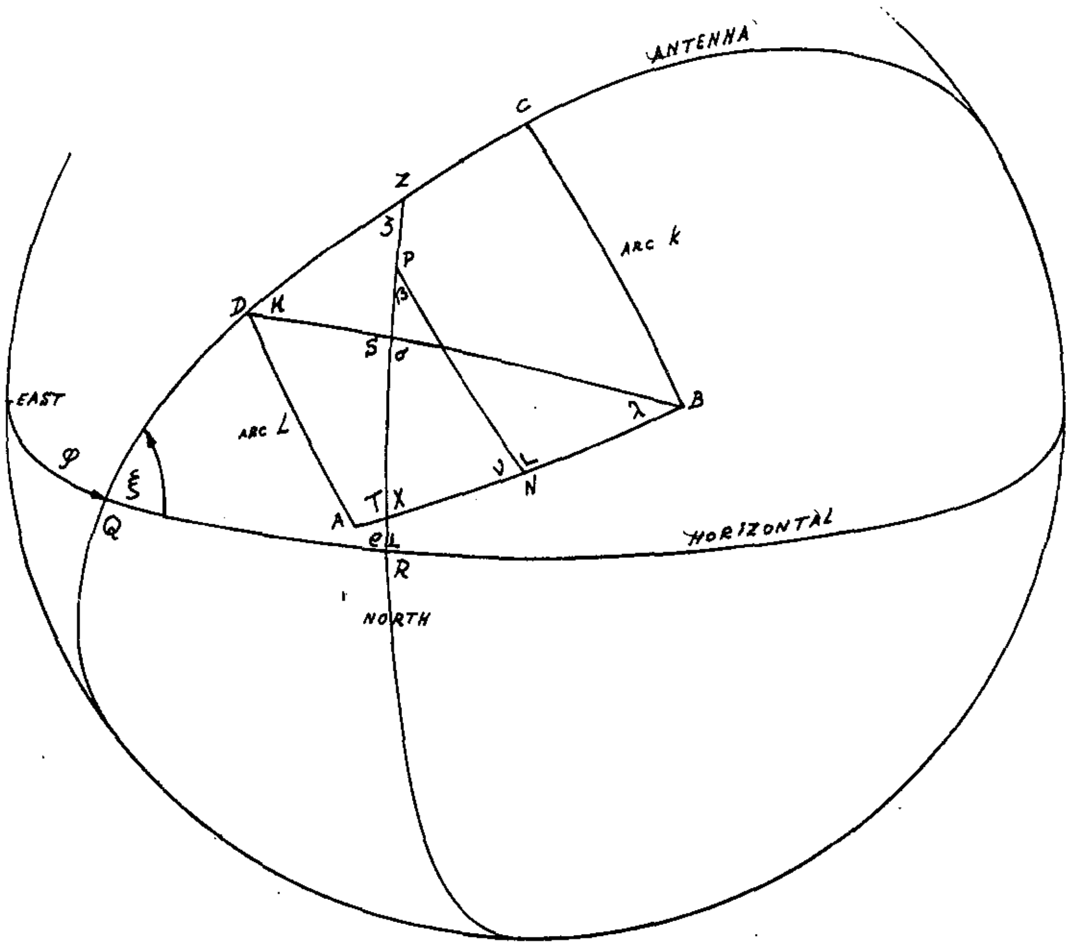

Fig. 12 All points A, B, C .... Z are lying on a sphere with centre M. The lines AD, BC etc. are arcs, being the projections of the straight lines AD, BC etc.

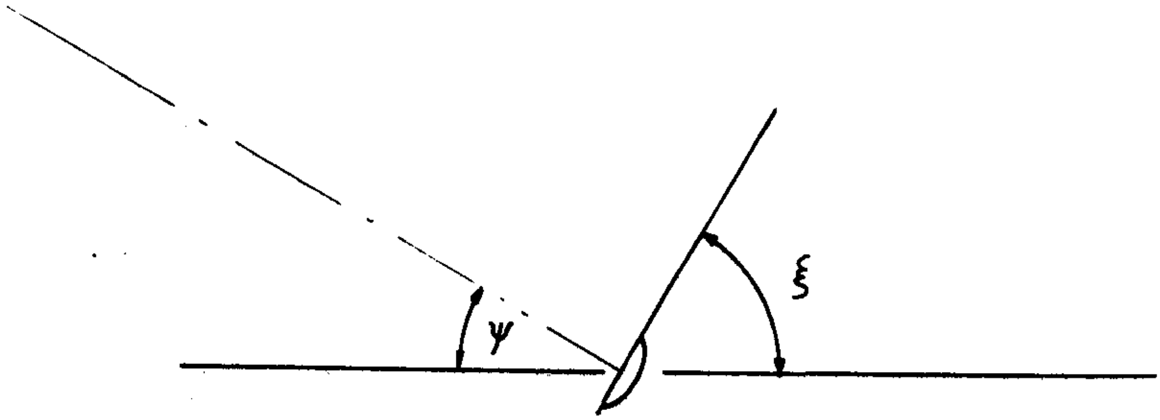

Fig. 13 ξ is the complement of the elevation ψ.

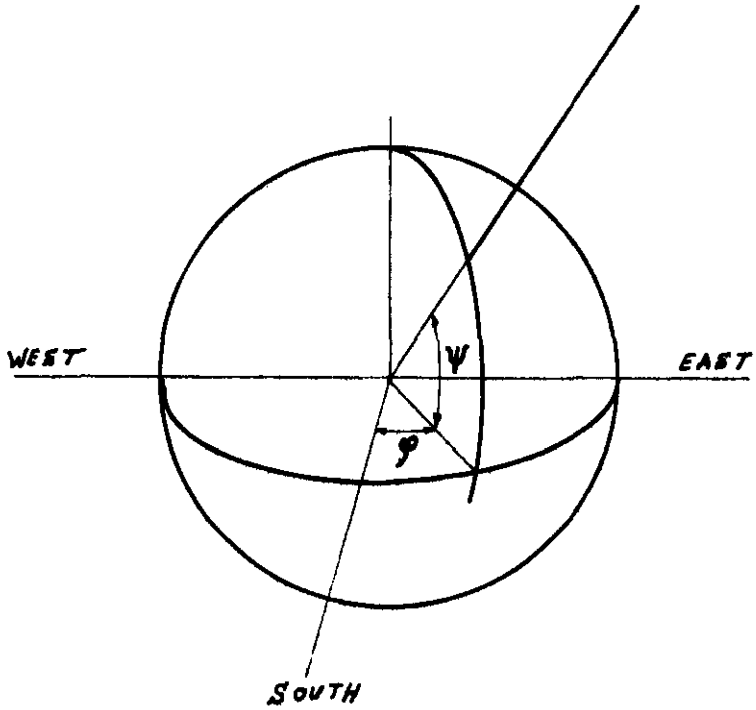

Fig. 14 Azimuth ϕ is related to the south, elevation ψ is related to the horizontal plane.

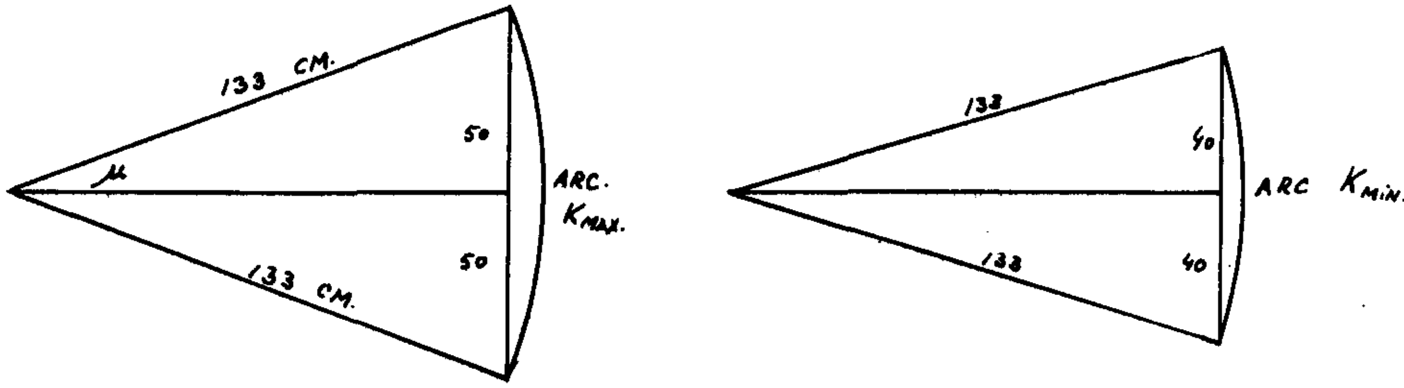

Fig. 15 The relation between the length of a lead screw and the arc projected on the ball surface of Fig. 12.

Fig. 16 The equatorial orbit and the reach of the antenna for $\beta = 27^{o}$ and $\beta = 0$.

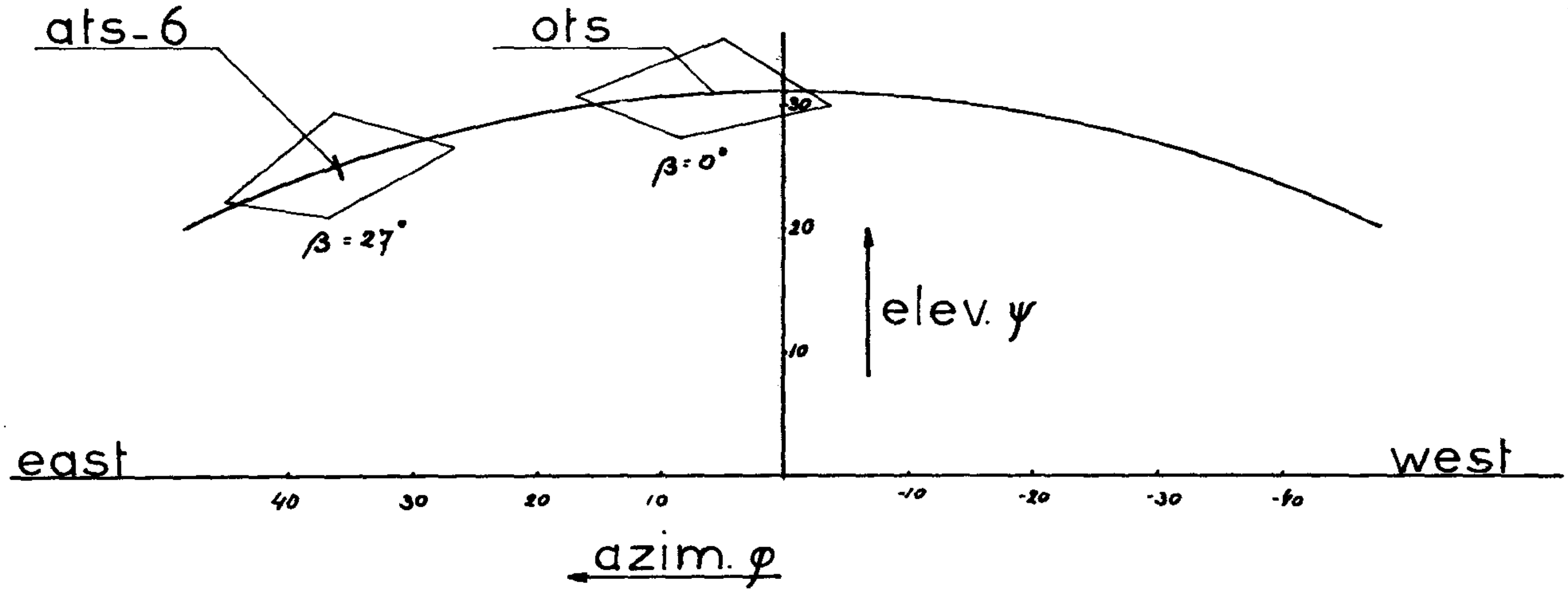

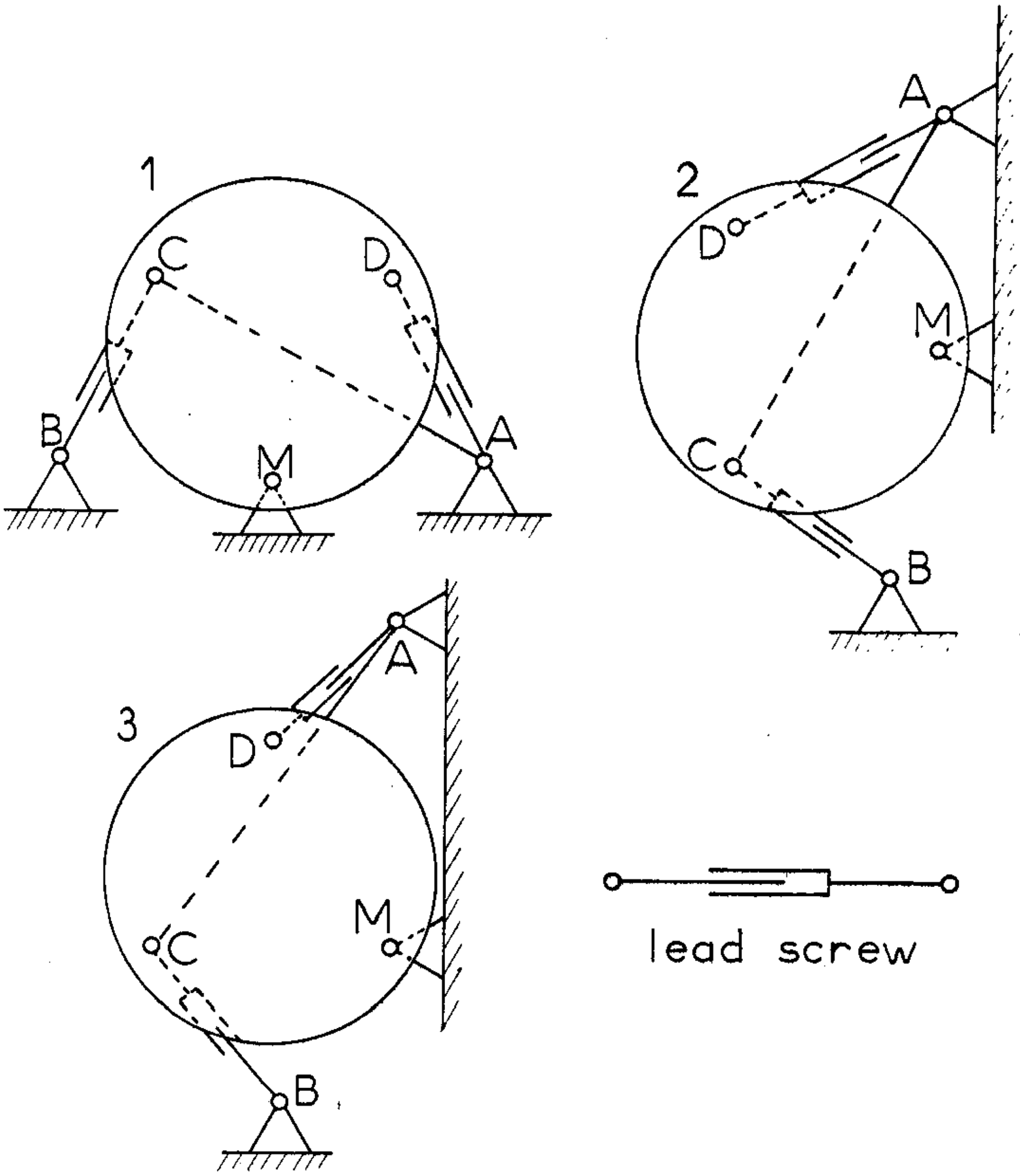

Fig. 17 Schematic suggestion to modify the Eindhoven mount into the ideal mount configuration.

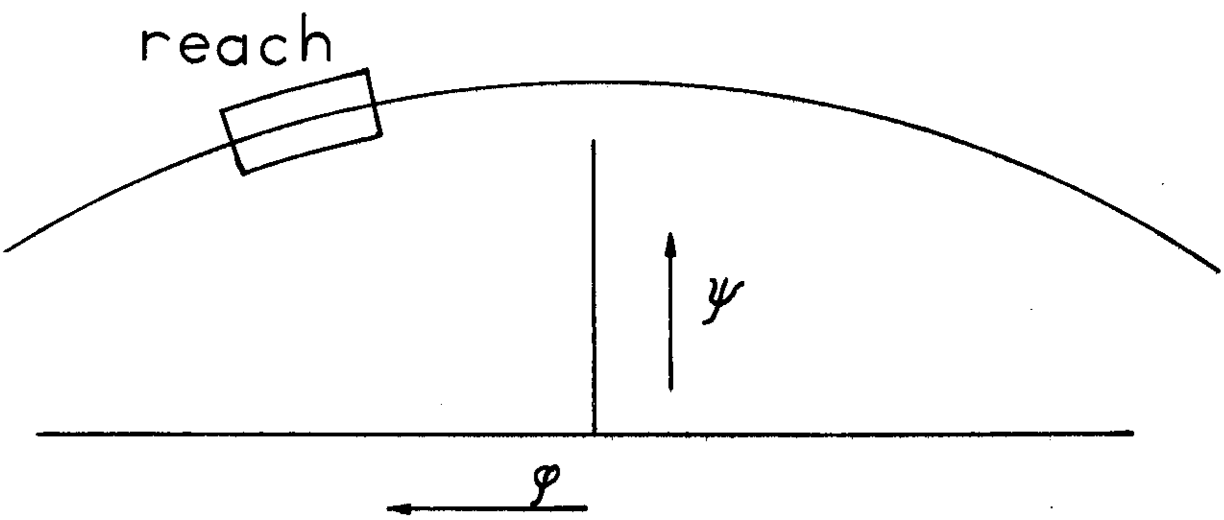

Fig. 18 The antenna reach in the equatorial orbit, using the ideal mount configuration.

EINDHOVEN UNIVERSITY OF TECHNOLOGY
THE NETHERLANDS
DEPARTMENT OF ELECTRICAL ENGINEERING

Reports:

1) Dijk, J., M. Jeuken and E.J. Maanders
AN ANTENNA FOR A SATELLITE COMMUNICATION GROUND STATION (PROVISIONAL ELECTRICAL DESIGN). TH-report 68-E-01. March 1968. ISBN 90 6144 001 7

2) Veefkind, A., J.H. Blom and L.H.Th. Rietjens
THEORETICAL AND EXPERIMENTAL INVESTIGATION OF A NON-EQUILIBRIUM PLASMA IN A MHD CHANNEL. TH-report 68-E-2. March 1968. Submitted to the Symposium on a Magnetohydrodynamic Electrical Power Generation, Warsaw, Poland, 24-30 July, 1968. ISBN 90 6144 002 5

3) Boom, A.J.W. van den and J.H.A.M. Melis
A COMPARISON OF SOME PROCESS PARAMETER ESTIMATING SCHEMES. TH-report 68-E-03. September 1968. ISBN 90 6144 003 3

4) Eykhoff, P., P.J.M. Ophey, J. Severs and J.O.M. Oome
AN ELECTROLYTIC TANK FOR INSTRUCTIONAL PURPOSES REPRESENTING THE COMPLEX-FREQUENCY PLANE. TH-report 68-E-04. September 1968. ISBN 90 6144 004 1

5) Vermij, L. and J.E. Daalder
ENERGY BALANCE OF FUSING SILVER WIRES SURROUNDED BY AIR. TH-report 68-E-05. November 1968. ISBN 90 6144 005 X

6) Houben, J.W.M.A. and P. Massee
MHD POWER CONVERSION EMPLOYING LIQUID METALS. TH-report 69-E-06. February 1969. ISBN 90 6144 006 8

7) Heuvel, W.M.C. van den and W.F.J. Kersten
VOLTAGE MEASUREMENT IN CURRENT ZERO INVESTIGATIONS. TH-report 69-E-07. September 1969. ISBN 90 6144 007 6

8) Vermij, L.
SELECTED BIBLIOGRAPHY OF FUSES. TH-report 69-E-08. September 1969. ISBN 90 6144 008 4

9) Westenberg, J.Z.
SOME IDENTIFICATION SCHEMES FOR NON-LINEAR NOISY PROCESSES. TH-Report 69-E-09. December 1969. ISBN 90 6144 009 2

10) Koop, H.E.M., J. Dijk and E.J. Maanders
ON CONICAL HORN ANTENNAS. TH-report 70-E-10. February 1970. ISBN 90 6144 010 6

11) Veefkind, A.
NON-EQUILIBRIUM PHENOMENA IN A DISC-SHAPED MAGNETOHYDRODYNAMIC GENERATOR. TH-report 70-E-11. March 1970. ISBN 90 6144 011 4

12) Jansen, J.K.M., M.E.J. Jeuken and C.W. Lambrechtse
THE SCALAR FEED. TH-report 70-E-12. December 1969. ISBN 90 6144 012 2

13) Teuling, D.J.A.
ELECTRONIC IMAGE MOTION COMPENSATION IN A PORTABLE TELEVISION CAMERA. TH-report 70-E-13. 1970. ISBN 90 6144 013 0

14) Lorencin, M.
AUTOMATIC METEOR REFLECTIONS RECORDING EQUIPMENT. TH-report 70-E-14. November 1970. ISBN 90 6144 014 9

15) Smets, A.J.
THE INSTRUMENTAL VARIABLE METHOD AND RELATED IDENTIFICATION SCHEMES. TH-report 70-E-15. November 1970. ISBN 90 6144 015 7

EINDHOVEN UNIVERSITY OF TECHNOLOGY
THE NETHERLANDS
DEPARTMENT OF ELECTRICAL ENGINEERING

Reports:

16) White, Jr., R.C.
A SURVEY OF RANDOM METHODS FOR PARAMETER OPTIMIZATION.
TH-report 70-E-16. February 1971. ISBN 90 6144 016 5

17) Talmon, J.L.
APPROXIMATED GAUSS-MARKOV ESTIMATORS AND RELATED SCHEMES.
TH-report 71-E-17. February 1971. ISBN 90 6144 017 3

18) Kalášek, V.
MEASUREMENT OF TIME CONSTANTS ON CASCADE D.C. ARC IN NITROGEN.
TH-report 71-E-18. February 1971. ISBN 90 6144 018 1

19) Hosselet, L.M.L.F.
OZONBILDUNG MITTELS ELEKTRISCHER ENTLADUNGEN.
TH-report 71-E-19. March 1971. ISBN 90 6144 019 X

20) Arts, M.G.J.
ON THE INSTANTANEOUS MEASUREMENT OF BLOODFLOW BY ULTRASONIC MEANS.
TH-report 71-E-20. May 1971. ISBN 90 6144 020 3

21) Roer, Th.G. van de
NON-ISO THERMAL ANALYSIS OF CARRIER WAVES IN A SEMICONDUCTOR.
TH-report 71-E-21. August 1971. ISBN 90 6144 021 1

22) Jeuken, P.J., C. Huber and C.E. Mulders
SENSING INERTIAL ROTATION WITH TUNING FORKS.
TH-report 71-E-22. September 1971. ISBN 90 6144 022 X

23) Dijk, J. and E.J. Maanders
APERTURE BLOCKING IN CASSEGRAIN ANTENNA SYSTEMS. A REVIEW.
TH-report 71-E-23. September 1971. ISBN 90 6144 023 8

24) Kregting, J. and R.C. White, Jr.
ADAPTIVE RANDOM SEARCH.
TH-report 71-E-24. October 1971. ISBN 90 6144 024 6

25) Damen, A.A.H. and H.A.L. Piceni
THE MULTIPLE DIPOLE MODEL OF THE VENTRICULAR DEPOLARISATION.
TH-report 71-E-25. October 1971. ISBN 90 6144 025 4

26) Bremmer, H.
A MATHEMATICAL THEORY CONNECTING SCATTERING AND DIFFRACTION PHENOMENA, INCLUDING BRAGG-TYPE INTERFERENCES.
TH-report 71-E-26. December 1971. ISBN 90 6144 026 2

27) Bokhoven, W.M.G. van
METHODS AND ASPECTS OF ACTIVE-RC FILTERS SYNTHESIS.
TH-report 71-E-27. 10 December 1970. ISBN 90 6144 027 0

28) Boeschoten, F.
TWO FLUIDS MODEL REEXAMINED.
TH-report 72-E-28. March 1972. ISBN 90 6144 028 9

29) REPORT ON THE CLOSED CYCLE MHD SPECIALIST MEETING. Working group of the joint ENEA/IAEA international MHD liaison group. Eindhoven, The Netherlands, September 20-22, 1971. Edited by L.H.Th. Rietjens.
TH-report 72-E-29. April 1972. ISBN 90 6144 029 7

EINDHOVEN UNIVERSITY OF TECHNOLOGY
THE NETHERLANDS
DEPARTMENT OF ELECTRICAL ENGINEERING

Reports:

30) Kessel, C.G.M. van and J.W.M.A. Houben
LOSS MECHANISMS IN AN MHD GENERATOR.
TH-report 72-E-30. June 1972. ISBN 90 6144 030 0

31) Veefkind, A.
CONDUCTING GRIDS TO STABILIZE MHD GENERATOR PLASMAS AGAINST IONIZATION INSTABILITIES. TH-report 72-E-31. September 1972.
ISBN 90 6144 031 9

32) Daalder, J.E. and C.W.M. Vos
DISTRIBUTION FUNCTIONS OF THE SPOT DIAMETER FOR SINGLE- AND MULTI-CATHODE DISCHARGES IN VACUUM. TH-report 73-E-32.
January 1973. ISBN 90 6144 032 7

33) Daalder, J.E.
JOULE HEATING AND DIAMETER OF THE CATHODE SPOT IN A VACUUM ARC.
TH-report 73-E-33. January 1973. ISBN 90 6144 033 5

34) Huber, C.
BEHAVIOUR OF THE SPINNING GYRO ROTOR.
TH-report 73-E-34. February 1973. ISBN 90 6144 034 3

35) Bastian, C. et al.
THE VACUUM ARC AS A FACILITY FOR RELEVANT EXPERIMENTS IN FUSION RESEARCH. Annual Report 1972. EURATOM-T.H.E. Group "Rotating Plasma".
TH-report 73-E-35, February 1973. ISBN 90 6144 035 1

36) Blom, J.A.
ANALYSIS OF PHYSIOLOGICAL SYSTEMS BY PARAMETER ESTIMATION TECHNIQUES. 73-E-36. May 1973. ISBN 90 6144 036 X

37) deleted

38) Andriessen, F.J., W. Boerman and I.F.E.M. Holtz
CALCULATION OF RADIATION LOSSES IN CYLINDRICAL SYMMETRICAL HIGH PRESSURE DISCHARGES BY MEANS OF A DIGITAL COMPUTER.
TH-report 73-E-38. October 1973. ISBN 90 6144 038 6

39) Dijk, J., C.T.W. van Diepenbeek, E.J. Maanders and L.F.G. Thurlings
THE POLARIZATION LOSSES OF OFFSET ANTENNAS.
TH-report 73-E-39. June 1973. ISBN 90 6144 039 4

40) Goes, W.P.
SEPARATION OF SIGNALS DUE TO ARTERIAL AND VENOUS BLOOD FLOW IN THE DOPPLES SYSTEM THAT USES CONTINUOUS ULTRASOUND.
TH-report 73-E-40. September 1973. ISBN 90-6144-040-8

41) Damen, A.A.H.
COMPARATIVE ANALYSIS OF SEVERAL MODELS OF THE VENTRICULAR DE-POLARISATION; INTRODUCTION OF A STRING-MODEL.
TH-report 73-E-41. October 1973. ISBN 90-6144-041-6

42) Dijk, G.H.M. van
THEORY OF GYRO WITH ROTATING GIMBAL AND FLEXTURAL PRIOTS.
TH-report 73-E-42. November 1973. ISBN 90-6144-042-4

EINDHOVEN UNIVERSITY OF THECHNOLOGY
THE NETHERLANDS
DEPARTMENT OF ELECTRICAL ENGINEERING

Reports:

43) Breimer, A.J.
ON THE IDENTIFICATION OF CONTINOUS LINEAR PROCESSES.
TH-report 74-E-43. January 1974. ISBN 90-6144-043-2

44) Lier, M.C.van and R.H.J.M. Otten
CAD OF MASKS AND WIRING.
TH-report 74-E-44. February 1974. ISBN 90-6144-044-0

45) Bastian, C. et al.
EXPERIMENTS WITH A LARGE SIZED HOLLOW CATHODE DISCHARGE FED WITH ARGON. Annual Report 1973. EURATOM-T.H.E. Group "Rotating Plasma".
TH-Report 74-E-45. April 1974. ISBN 90-6144-045-9

46) Roer, Th.G. van de
ANALYTICAL SMALL-SIGNAL THEORY OF BARITT DIODES.
TH-report 74-E-46. May 1974. ISBN 90-6144-046-7

47) Leliveld, W.H.
THE DESIGN OF A MOCK CIRCULATION SYSTEM.
TH-report 74-E-47. June 1974. ISBN 90-6144-047-5

48) Damen, A.A.H.
SOME NOTES ON THE INVERSE PROBLEM IN ELECTRO CARDIOGRAPHY.
TH-report 74-E-48. July 1974. ISBN 90-6144-048-3

49) Meeberg, L. van de
A VITERBI DECODER.
TH-report 74-E-49. October 1974. ISBN 90-6144-049-1

50) Poel, A.P.M. van der
A COMPUTER SEARCH FOR GOOD CONVOLUTIONAL CODES.
TH-report 74-E-50. October 1974. ISBN 90-6144-050-5

51) Sampic, G.
THE BIT ERROR PROBABILITY AS A FUNCTION PATH REGISTER LENGTH IN THE VITERBI DECODER.
TH-report 74-E-51. October 1974. ISBN 90-6144-051-3

52) Schalkwijk, J.P.M.
CODING FOR A COMPUTER NETWORK.
TH-report 74-E-52. October 1974. ISBN 90-6144-052-1

53) Stapper, M.
MEASUREMENT OF THE INTENSITY OF PROGRESSIVE ULTRASONIC WAVES BY MEANS OF RAMAN-NATH DIFRACTION.
TH-report 74-E-53. November 1974. ISBN 90-6144-053-X

54) Schalkwijk, J.P.M. and A.J. Vinck
SYNDROME DECODING OF CONVOLUTIONAL CODES.
TH-report 74-E-54. November 1974. ISBN 90-6144-054-8

55) YAKIMOV, A.
FLUCTUATIONS IN IMPATT-DIODE OSCILLATORS WITH LOW q-SECTORS.
TH-report 74-E-55. November 1974. ISBN 90-6144-054-6

EINDHOVEN UNIVERSITY OF TECHNOLOGY
THE NETHERLANDS
DEPARTMENT OF ELECTRICAL ENGINEERING

Reports:

56) Plaats, J. van der
ANALYSIS OF THREE CONDUCTOR COAXIAL SYSTEMS.
TH-report 75-E-56. March 1975. ISBN 90-6144-056-4

57) Kooy, C.
RE-OPTICAL ANALYSIS OF A TWO DIMENSIONAL APERTURE RADIATION
PROBLEM. TH-report 75-E-57. April 1975. ISBN 90-6144-057-2

58) Schalkwijk, J.P.M., A.J. Vinck and L.J.A.E. Rust
ANALYSIS AND SIMULATION OF A SYNDROME DECODER FOR A CONSTRAINT
LENGTH k = 5, RATE R = ½ BINARY CONVOLUTIONAL CODE.
TH-report 75-E-58. April 1975. ISBN 90-6144-058-0

59) Boeschoten, F. et al.
EXPERIMENTS WITH A LARGE SIZED HOLLOW CATHODE DISCHARGE FED
WITH ARGON, II. Annual Report 1974. EURATOM-T.H.E. Group
"Rotating Plasma". TH-report 75-E-59. June 1975. ISBN 90-6144-059-9

60) Maanders, E.J.
SOME ASPECTS OF GROUND STATION ANTENNAS FOR SATELLITE COMUNICATION.
TH-report 75-E-60. August 1975. ISBN 90-6144-060-2
(This report has served as a thesis for the degree of Doctor of
Applied Science at the University of Gent, Belgium, 1975)

61) Mawira, A. and J. Dijk
DEPOLARIZATION BY RAIN: Some Related Thermal Emission Considerations.
TH-report 75-E-61. September 1975. ISBN 90-6144-061-0

62) Safak, M.
CALCULATION OF THE RADIATION PATTERNS OF PARABOLOIDAL REFLECTORS
BY HIGH FREQUENCY ASYMPTOTIC TECHNIQUES.
TH-report 76-E-62. March 1976. ISBN 90-6144-062-9

63) Schalkwijk, J.P.M. and A.J. Vinck
SOFT DECISION SYNDROME DECODING.
TH-report 76-E-63. March 1976. ISBN 90-6144-063-7

64) Damen, A.A.H.
EPICARDIAL POTENTIALS DERIVED FROM SKIN POTENTIAL MEASUREMENTS.
TH-report 76-E-64. July 1976. ISBN 90-6144-064-5

65) Bakhuizen, A.J.C. and R. de Boer
ON THE CALCULATION OF PERMEANCES AND FORCES BETWEEN DOUBLY SLOTTED
STRUCTURES.
TH-report 76-E-65. September 1976. ISBN 90-6144-065-3

66) Geutjes, A.J.
A NUMERICAL MODEL TO EVALUATE THE BEHAVIOUR OF A REGENERATIVE HEAT
EXCHANGER AT HIGH TEMPERATURE.
TH-report 76-E-66. November 1976. ISBN 90-6144-0661

67) Boeschoten, F. et al.
EXPERIMENTS WITH A LARGE SIZED HOLLOW CATHODE DISCHARGE, III; concluding
work Jan. 1975 to June 1976 of the EURATOM-THE Group "Rotating Plasma".
TH-report 76-E-67. November 1976. ISBN 90-6144-067-X

EINDHOVEN UNIVERSITY OF TECHNOLOGY
THE NETHERLANDS
DEPARTMENT OF ELECTRICAL ENGINEERING

Reports:

68) Boeschoten, F. and R. Komen
ISOTOPE SEPARATION WITH A HOLLOW CATHODE DISCHARGE.
TH-report 76-E-68. December 1976. ISBN 90-6144-068-8

69) Merck, W.F.H. and A.F.C. Sens
THOMSON-SCATTERING MEASUREMENTS ON A HOLLOW CATHODE DISCHARGE.
TH-report 76-E-69. December 1976. ISBN 90-6144-069-6

70) Jongbloed, A.A.
STATISTICAL REGRESSION AND DISPERSION RATIOS IN NONLINEAR SYSTEM IDENTIFICATION.
TH-report 77-E-70. March 1977. ISBN 90-6144-070-X

71) Barrett, J.F.
BIBLIOGRAPHY ON VOLTERRA SERIES HERMITE FUNCTIONAL EXPANSIONS AND RELATED SUBJECTS.
TH-report 77-E-71. March 1977. ISBN 90-6144-071-8